Geological Journal

Oscillations of a fluvial-lacustrine system and its ecological response prior to the end-Triassic: evidence from the eastern Tethys region

Journal:	*Geological Journal*
Manuscript ID	GJ-22-0422.R1
Wiley - Manuscript type:	Research Article
Date Submitted by the Author:	06-Nov-2022
Complete List of Authors:	Wang, Yongdong; Nanjing Institute of Geology and Palaeontology Chinese Academy of Sciences; University of Chinese Academy of Sciences, Nanjing College Lu, Ning; Nanjing Institute of Geology and Palaeontology Chinese Academy of Sciences Xu, Yuanyuan; Nanjing Institute of Geology and Palaeontology Chinese Academy of Sciences; University of Chinese Academy of Sciences Li, Liqin; Nanjing Institute of Geology and Palaeontology Chinese Academy of Sciences Xie, Xiaoping; Qufu Normal University Popa, Mihai ; Southwest Petroleum University; University of Bucharest, Faculty of Geology and Geophysics, Doctoral School of Geology, Laboratory of Palaeontology Chen, Hongyu; Nanjing Institute of Geology and Palaeontology Chinese Academy of Sciences; University of Chinese Academy of Sciences Ruhl, Micha; Trinity College Dublin The University of Dublin, Department of Geology Kürschner, Wolfram Michael; Universitetet i Oslo
Keywords:	sedimentary oscillations, floral community succession, Central Atlantic Magmatic Province, end-Triassic mass extinction, Sichuan Basin

Oscillations of a fluvial-lacustrine system and its ecological response prior to the end-Triassic: evidence from the eastern Tethys region

Ning Lu [1], Yongdong Wang [1,8*], Yuanyuan Xu [1,7], Liqin Li [1], Xiaoping Xie [4], Mihai Emilian Popa [2,3*], Hongyu Chen [1,7], Micha Ruhl [5], Wolfram Michael Kürschner [6]

[1]State Key Laboratory of Palaeobiology and Stratigraphy, Nanjing Institute of Geology and Palaeontology, Chinese Academy of Sciences, Nanjing 210008, China

[2]School of Geosciences and Technology, Southwest Petroleum University, Chengdu 610500, China

[3]University of Bucharest, Faculty of Geology and Geophysics, Doctoral School of Geology, Laboratory of Palaeontology, 1, N. Bălcescu Ave, Bucharest 010041, Romania

[4]School of Geography and Tourism, Qufu Normal University, Rizhao 276826, China

[5]Department of Geology, Trinity College Dublin, The University of Dublin, College Green, Dublin 2, Ireland

[6]Department of Geosciences, University of Oslo, N-0316 Oslo, Norway

[7]University of Chinese Academy of Sciences, Beijing 100049, China

[8]Nanjing College, University of Chinese Academy of Sciences, Nanjing 210006, China

*** Correspondence:**

Yongdong Wang: ydwang@nigpas.ac.cn

Mihai Emilian Popa: mihai@mepopa.com

Abstract

The end-Triassic mass extinction is considered as one of the “Big Five” extinction events in the Phanerozoic. However, whether the terrestrial ecosystem began to deteriorate or even collapse prior to the Triassic–Jurassic transition remains controversial. Compared with the documented data from the western Tethyan region, evidence from the eastern Tethyan realm is limited. We undertake a fitting analysis of the sedimentary system, floral community successions and major geological events of the Xujiahe Formation as reflected by the Qilixia Section, Xuanhan area, northeast Sichuan Basin, China. Our results reveal an oscillating fluvial-lacustrine depositional system during the Late Triassic, with the dominant sedimentary processes mainly controlled by the Indosinian Movement. Beside the sedimentary influence on the Xujiahe Flora, climate changes played a more important role. Fluctuating conditions to cooler and dryer climates at this time promoted diversification of gymnosperms under an overall warm and humid climate setting in the Late Triassic in the Xuanhan area. Superimposed on this oscillating long-term climate state, ecosystem destabilization occurred over one million years prior to the Tr–J interval in the Xuanhan study-area, possibly in response to the intensified storm and wildfire activity and the following environmental changes. Although the Xujiahe Flora always recover from the interruption of the tectonic movement, it ultimately collapsed under extreme climatic events and ecological pressures induced by the Late Triassic CAMP event.

Keywords: sedimentary oscillations, floral community succession, Central Atlantic Magmatic Province, end-Triassic mass extinction, Sichuan Basin.

1 Introduction

The Triassic-Jurassic transition (Tr–J, 201.36 ± 0.17 Ma, Wotzlaw et al., 2014) is marked by the end-Triassic mass extinction, one of the "Big Five" extinction events of the Phanerozoic (Sepkoski, 1981; Raup and Sepkoski, 1982; Benton, 1995). The biotic turnover, ecological crisis, and environmental background across the Tr–J transition have drawn significant attention over the last decades (Hesselbo et al., 2007; Barash, 2015). The impact of the end-Triassic mass extinction on marine organisms has been extensively documented (e.g., radiolarians, Hallam, 2002; foraminifera, Michalík et al., 2007; ammonites and brachiopods, Tomašových and Siblík, 2007; corals and calcisponges, Stanley et al., 2018; bivalves, Atkinson et al., 2019). Bio- and chemo-stratigraphic data and stratigraphic correlations of sea-level changes, ocean acidification and release of greenhouse gases (e.g., CO_2, CH_4) suggest this event to be triggered by the breakup of Pangea and particularly by the eruptions of the Central Atlantic Magmatic Province (CAMP) at that time (Marzoli et al., 2004; Van de Schootbrugge et al., 2009; Whiteside et al., 2010; Ruhl et al., 2011, 2020; Percival et al., 2017; Capriolo et al., 2020; He et al., 2020). Extreme climatic events caused by significant global warming led to habitat and ecosystem disruption and destruction, with palynological and geochemical data suggesting this to have occurred simultaneously in the terrestrial and marine realms (McElwain et al., 1999; Hesselbo et al., 2002; Cleveland et al., 2008; Götz et al., 2009; Williford et al., 2009; Korte et al., 2019). However, the extinction patterns across this event remain controversial, with some suggestions for multiple extinction events throughout the Late Triassic instead of a single mass extinction at the end of the Late Triassic (Benton, 1986; Hallam, 2002; Lucas and Tanner, 2015, 2018). Considerable controversy derives from the response of terrestrial vegetation to these events. Studies of the plant taxonomic records from Greenland, North America, Europe and Gondwana revealed a significant floral turnover at species and community levels (Fowell and Olsen, 1993; McElwain et al., 1999; Olsen et al., 2002; McElwain and Punysasena, 2007; Küerschner et al., 2007; Belcher et al., 2010; Kustatscher et al., 2018). Other works considered that plant community changes across the Tr–J transition were linked to gradual and adaptive ecological reorganization related to long-term environmental variations, suggesting terrestrial plant changes to be local turnovers rather than associated with a mass extinction (Cascales-Miňana and Cleal, 2012; Barbacka et al. 2017; Lucas and Tanner, 2018; Zhou et al., 2021). As most studies on the end-Triassic mass extinction were carried out in the western Tethyan realm, especially in Europe and North America, critical insight on global changes, including as recorded in the eastern Tethyan realm is largely missing.

Terrestrial Tr–J transition sequences are well developed in the Sichuan Basin, southwestern China, representing the most expanded Tr–J strata in the eastern Tethyan realm (Wang et al., 2010). Fundamental studies on regional geology, stratigraphy and palaeontology were previously conducted (Wang et al., 2010), showing abundant yields of diverse plant fossils, represented by the Xujiahe Flora, in the Upper Triassic sequences of the Sichuan Basin (Ye et al., 1986; Huang, 1995; Wang et al., 2010). The Xujiahe Flora has been suggested to be flourishing under a tropical-subtropical hot and humid climatic conditions (Lee, 1964; Ye et al., 1986; Wu, 1983; Sun, 1995). In recent years, studies on systematic palaeobotany (Wang et al., 2015; Lu et al., 2021; Xu et al., 2021), palynology (Liu et al., 2015; Li et al., 2016, 2018), as well as sedimentology and geochemistry (Zhu et al., 2017; Pole et al., 2018; Lu et al., 2019; Shen et al., 2022) were conducted for these Upper Triassic sequences of the Sichuan Basin, showing notable temporal variations in climate at that time (Tian et al., 2016; Lu et al., 2019; Li et al., 2020; Li et al., 2021). The environmental evolution during the Late Triassic in the northeastern Sichuan Basin is yet poorly understood, it is critical to provide insight on the level of ecosystem stability, deterioration and/or collapse prior to the Tr–J transition in this region.

Here, we investigate the sedimentary succession and sedimentary features of the Upper Triassic sequences in the northeastern Sichuan Basin, with the emphasis on the significance of the macro- and micro-floral records related to their depositional context. We aim to reveal the environmental/climatic oscillations and ecological responses during the Rhaetian (Late Triassic) in the northeastern Sichuan Basin, next to discussion on the wider stability of terrestrial ecosystem prior to the Tr–J transition.

2 Geological Settings

The Sichuan Basin occurred on the northern frame of the eastern Tethyan realm (Fig. 1-A). This basin is one of the largest sedimentary basins in southwestern China, covering the eastern Sichuan Province and the majority of Chongqing City (Fig. 1-B). Its tectonic evolution can be divided into three stages: basement formation, craton basin and foreland basin (Wang et al., 2010). The igneous basement of the Sichuan Basin is Meso-Neoproterozoic in age. The sedimentary cover of the Sichuan Basin recorded a stable craton development stage, reflected by a set of shallow platform carbonate deposits. When the South China Block, the North China Block and the Songpan-Ganzi Terrane collided during the Late Triassic, the Sichuan foreland basin was formed, and the depositional environment changed from marine to terrestrial (Wang et al., 2010). During this time interval, both the end-Triassic mass extinction and the long-term formation of the Sichuan Basin were accurately, and continuously recorded in the Upper Triassic deposits.

The Upper Triassic sequences of the Sichuan Basin are represented by the Xujiahe Formation, a succession of clastic rocks with abundant coal and gas resources (Wang et al., 2010). The formation is widely distributed and well outcropped in the eastern and northeastern margins of the basin. The Qilixia Section is one of the key and well-known Upper Triassic-Lower Jurassic sections in this area, occurring close to Qili town in Xuanhan County, Dazhou City (Figs. 1-B, C). The Xujiahe Formation is about 520 m thick, outcropping along the road from Xuanhan to Kaijiang counties. The Xujiahe Formation unconformably overlies the Middle Triassic Leikoupo Formation and it is conformably overlain by the Lower Jurassic Zhenzhuchong Formation. The Xujiahe Formation is divided into seven members (Members I–VII) with distinct lithological boundaries between each member (Wang et al., 2010). Previous palaeobotanical and palynological data suggest that the Xujiahe Formation is

Norian to Rhaetian in age (Ye et al., 1986; Li et al., 2016, 2018, 2020). The combined cyclo- and magneto-stratigraphic record for this section and formation demonstrate that the age of the Xujiahe Formation spans from the latest Norian to the Rhaetian, i.e., from 207.2 Ma to 201.3 Ma (Li et al., 2017).

(Fig. 1 is approximately here)

3 Material and Methods

The Qilixia Section was here studied and sampled for sedimentological investigations. Facies analyses were conducted according to precise sequence data and sedimentary features (Figs. 2-4).

Published plant macrofossils of the Xujiahe Formation at the Qilixia Section were compiled and analyzed, revealing their ecology (Ye et al., 1986; Wu, 1999; Wang et al., 2010; Lu, 2019), and new plant specimens were collected and supplemented to the previously existing dataset, next to sporomorph data (Li et al., 2016, 2020; Lu et al., 2020).

Photographs of plant fossils were taken with a Nikon® Z7 digital camera with an Z 24-70mm f/4 S lens. The photographs of plant fossils and lithologies of the Xujiahe Formation were corrected only for contrast and sharpness using Adobe® Photoshop®. The line drawings of some plant fossils were produced using CorelDRAW® 2021. The selected specimens of plant fossils reported and figured here are housed in the Nanjing Institute of Geology and Palaeontology, Chinese Academy of Sciences, Nanjing, China with catalogue numbers: QLX2014103, QLX2014146, QLX2014159, QLX2014163, QLX2014170, QLX2014350, QLX2014399, QLX-2105-15U-542.

4 Results

4.1 Lithology

The Xujiahe Formation comprises seven lithological members (Members I-VII) in the studied section. Stratigraphic boundaries between each member and bed are distinct and they are easily recognized through lithological features (Figs. 2-A, B). The Xujiahe Formation is represented by a succession of dominant sandstone and mudstone beds, while, conglomerates, coal seams and thin layers of concretions were also deposited. Rock colors, sedimentary structures, coal accumulation and fossil preservation further reflect the Late Triassic depositional features.

(Fig. 2 is approximately here)

The members II, IV and VI of the Xujiahe Formation are dominated by thick sandstone beds, mostly medium to fine grained feldspathic-quartz and quartz sandstone, showing grayish to gray colors (Fig. 2-C). Carbonized plant branches are preserved in these sandstone beds (Fig. 2-D). A few coarse sandstone layers occur with quartz and/or chert gravels and with erosional surfaces (Fig. 3-A). Cross bedding is the most frequent and notable structure in the sandstone beds, usually associated with parallel bedding as well (Figs. 3-B, C). Climbing ripples are recorded in the members II and IV (Fig. 3-D). Wave-ripple marks and load-casts occur in the sandstone of the members II and VI (Figs. 3-E, F).

The members I, III, V and VII are dominated by gray to black mudstone and silty mudstone beds (Figs. 2-A, E, F). Variations in colors, between ‘grey’, ‘dark grey’ and ‘black’ are mainly dependent on the organic matter content, beds of these colors were mostly deposited in a coastal marsh (e.g., Member I) or peat swamp (e.g., Member VII), co-existing with coal seams. The horizontal and massive beddings of the mudstone beds are typically indicative for changing hydrodynamics and for supply of terrestrial clastics. Mudstones with preserved root-mucks and mud-cracks in Member I suggest that unconsolidated sediments were once exposed to relatively dry climate conditions (Figs. 3-G, 5-A). The *Skolithos*-type burrows of the Member III show a near-shore environment (Fig. 3-H). Some thin layers of siderite concretions are exposed in the mudstone beds of members I and V (Fig. 2-E), and two layers of calcic concretions are developed to the top of Member I.

(Fig. 3 is approximately here)

Conglomerate layers are exposed to the bottom of the sandstone beds, and some conglomerate lenses occur within sandstone beds (Figs. 2-G, 3-A). Quartzite and chert pebbles are common in conglomerate layers, indicating a long distance of transportation and/or flushing effects of high-energy flow. Fossil tree trunks are common observed in the conglomerate layers, as a result of flash flooding, debris flow events (Fig. 2-H).

Multiple thin coal seams occur in the mudstone members I, III, V and VII (Figs. 2-A, F), suggesting a reducing environment with abundant clastic sediments. The main industrial coal seams occur in Member VII (Fig. 2-F), and few coal seams of the Member V have also mining significance. Particular thin layers of siltstone and muddy siltstone occur as roof and floor shales.

4.2 Sedimentary facies and environment

The Xujiahe Formation of the Qilixia Section records a fluvial and lacustrine system (Fig. 4), while Member I records also a coastal marsh depositional system. These systems could be identified based on facies, subfacies and microfacies characters.

(Fig. 4 is approximately here)

The sandstone members record a well-developed meandering river system (e.g., members II and IV, Fig. 4). Associated riverbed microfacies is mainly represented by conglomerate and pebbly sandstone with clear erosional surfaces (e.g., the middle part of bed 04, Member II, Fig. 4). The typical retention sediments, including tree trunks and mud inclusions, are usually exposed as lenses to the bottom of erosional surfaces (Fig. 3-A). The marginal bank (point bar) microfacies is mainly represented by grayish, cross-bedded sandstone (e.g., the upper part of bed 04, Member II, Fig. 4). The levee microfacies is developed upward along the marginal banks, depositing fine-grained sandstone and siltstone. Flash floods destroyed levees and formed crevasse splay microfacies. Carbonized branches and mud interlayers are common in the sandstone beds of a crevasse splay (e.g., Fig. 2-D). The floodplain subfacies was generally developed to the top stage of a meandering river system or lateral it, consisting of siltstone and muddy siltstone. Horizontal beddings are common, and calcic concretions occur locally. The observed peat swamp was developed in a floodplain, with a limited preservation for channel lateral migration (e.g., bed 10, Member V, Fig. 4).

The fluvial delta plain facies expanded into a fluvial-lacustrine transition zone (e.g., Member V, Fig. 4). The distributary channel microfacies are mainly represented by fine-grained, well-sorted sandstone. Mud flames and tree trunks are common to the bottom of channel sandstone beds (e.g., bed 10, Member V, Fig. 4). The interdistributary bay microfacies are dominated by dark gray to black mudstone and carbonaceous mudstone, interlayered with thin-bedded siltstone. Plant fossils and siderite concretions are common in the interdistributary bay deposits (e.g., the lower part of bed 09, Member V, Fig. 4). Peat continuously accumulated in the swamps of a relatively stable delta plains, and which represents the important coal accumulating environments (e.g., the upper part of bed 09, Member V, Fig. 4).

The lacustrine system included of lakeshore and shallow lake subfacies (e.g., bed 16 and the lower part of bed 15, Member VII, Fig. 4). However, semi-deep and deep lake subfacies did not develop in the Qilixia Section locality. The lakeshore subfacies are dominated by gray-dark to black mudstone. Industrial coal seams were developed in the lakeshore swamp microfacies, containing fine-grained and thin bedded sandstone and siltstone beds (Fig. 2-F). The shallow lake subfacies are dominated by a thin-bedded gray mudstone, silty mudstone, and muddy siltstone. Some hydrophyte plant taxa (e.g., *Neocalamites*) and bivalves occur in the shallow lake deposits (Huang and Lu, 1992).

According to the occurrence of marine bivalve fossils in the western Sichuan Basin and to the occurrence of *Lingula* sp. in the eastern Sichuan Basin, the microfacies of Member I consists of lagoon, coastal marsh and estuarine sandbars (Gou, 1998; Wang et al., 2017; Fig. 4), as a result of the transgression and regression cycles during the latest Norian to the Rhaetian (Lu et al., 2015, 2019).

4.3 Floral community succession

The Xujiahe Flora has been reported throughout the Sichuan Basin, yielding well-preserved and highly diverse fossils, especially for the Qilixia Section and its surrounding areas (Ye et al., 1986; Wang et al., 2010; Fig. 5), counting 110 species of 59 genera of plant macrofossils (Ye et al., 1986;

Lu, 2019; Fig. 6, Table S1). Palynological studies of the Qilixia Section are extensive, reporting a high diversity of spores and pollen, counting 151 species of 64 genera (Li et al., 2016, 2020; Fig. 7).

(Figs. 5-8 are approximately here.)

Most of the plant fossils from Member I are too fragmentary to be investigated. According to palynological investigations, the dominant group of Member I are ferns (52.09~55.31%), followed by conifers (19.56~30.17%) and cycads/bennettites/ginkgophytes (8.94~14.97%) (Fig. 8). Some palynomorph environmental indicators (i.e., *Sulcusicystis* sp. and *Radicites* sp.) are also found in Member I (Lu et al., 2015; Li et al., 2016; Fig. 5-A), all indicating a coastal hydrophyte community (CHC) for Member I at this time (Fig. 6).

Plant macrofossils preserved in Member III suggest a community dominated by ferns, cycads, and horsetails (Fig. 6, Table S1). The palynological data also indicate the similar community composition, with dominant groups of ferns (51.06~64.33%) and cycads/bennettites/ginkgophytes (14.33~15.60%) (Fig. 8). The plant macrofossils and palynological data indicate a delta-plain wetland community (DWC) (Lu, 2019; Li et al., 2020). Compared with the CHC of Member I, the diversity of gymnosperms is higher in the DWC of Member III (Lu et al., 2019; Fig. 6).

Both macro- and micro-fossils are preserved in the lower beds of Member V (Figs. 5-C, D, E, F, and Fig. 8). However, the top of Member V yields only macrofossils and no palynomorphs (Fig. 8). The dominant groups include ferns (e.g., *Cladophlebis raciborskii*, *Todites* sp., Fig. 5-D, F), cycads (e.g., *Pterophyllum angustum*, Fig. 5-C), and ginkgophytes (e.g., *Ixostrobus* sp., Fig. 5-E). The proportion of fern spores is up to 71.78%, whereas the conifers is only 15.34% (sample QLX-10 of Bed 9, Member V; Fig. 8). Both the macro- and micro-fossils indicate a swamp wetland community (SWC) to have preserved in Member V (Lu, 2019; Li et al., 2020; Figs. 6 and 8).

Most fossil taxa of the Xujiahe Flora were found in Member VII, such as *Dictyophyllum nathorsti*, *Cladophlebis* sp., *Baiera elegans* and *Ginkgoites* sp. (Figs. 5-G, H, I, J). Both species and genera diversity of the plant macrofossils increase at first and then decrease (Fig. 6). The dominant groups changed from horsetails to ferns and cycads (Bed 15), and then to ginkgophytes and conifers (Bed 15 to 17) (Ye et al., 1986; Lu, 2019; Fig. 6). Meanwhile, the palynological data also show an upward decrease in ferns and an increase in gymnosperms (e.g., conifers, ginkgophytes) from Bed 15 to Bed 17 (Li et al., 2020; Fig. 8). This assemblage change reflects a transitional community succession (TCs), changing from lakeshore swamp to high lands that were preserved in Member VII (Figs. 6 and 8).

5 Discussion

5.1 Oscillations between fluvial and lacustrine depositional systems

Significant changes in term of palaeogeography, palaeoclimate and palaeoecology occurred in the Sichuan Basin throughout the Late Triassic. The Sichuan Basin occurred on the northern margin of the South China Block during the Late Triassic (Fig. 1-A). With the convergence of the South China Block, the North China Block, and the Indo-China Block (known as the Indosinian Movement), the Sichuan Basin was raised during the Middle- Late Triassic (Zhong et al., 1998). Due to the uplift of the Sichuan Basin, the westward retreat of the Tethys occurred and the Middle Triassic Leikoupo Formation was weathered during the Middle-Late Triassic in the Xuanhan area (Deng, 1996; Zhong et al., 1998; Wang et al., 2010). This large-scale regression was recorded by the sedimentary gap between the Middle Triassic Leikoupo Formation and the Upper Triassic Xujiahe Formation (Fig. 2-A).

Following the large-scale regression, a new transgressive episode started in the Carnian and influenced the Xuanhan area in the latest Norian (Lu et al., 2015). Thereafter, a coastal marsh began to take shape and the Xujiahe Formation deposited unconformably over the Leikoupo Formation remains (Fig. 2-A). Some thin layers of coal were accumulated, with the coincidental formation of calcic concretions and gypsum of Member I deposits, indicating a hot climate (Lu et al., 2015).

(Fig. 9 is approximately here)

With the continuous northward compression of the northern margin of the South China Block, the Qinling orogen to the north of the Sichuan Basin became raised and rivers originating from the Qinling orogen started to shape the topography of the Xuanhan area with sufficient terrigenous clastic sediments and water. The meandering rivers became the dominant sedimentary environment, as represented by the sequences of Member II. Repeated flood events, inferred from the regular occurrence of riverbed-point bar-natural levee associations, suggest regular heavy rain events in response to a megamonsoon development (Parrish and Peterson, 1988; Tian et al., 2016) (Fig. 9).

With the initial formation of the Sichuan Basin and the continuous deepening of the water at the study locality, the transition from channel to floodplain to lakeshore swamp was recorded in Member III (Figs. 4 and 9). However, the relatively stable environment didn't last long before the start of another episode of the Indosinian Movement (also known as the Anxian Movement, Wang, 1990). The tectonic activities not only promoted the continuous uplift of the Qinling Orogen, but also resulted in the uplift of the Longmenshan mountains, forming a prominent syntectonic conglomerate sequence near the source area (Wang, 2003; He, 2014; Liu et al., 2021). The fluvial dynamics of the surrounding orogens were therefore enhanced, providing sufficient terrigenous clastic sediments and water. The facies association of Member IV of the Qilixia Section recorded the Anxian Movement and its impact from a distance (Fig. 4).

With the tectonic activities tending to moderate, the environment became stable and the lake level became raised (Fig. 9). The wide deltaic flood-plain was formed in the middle Rhaetian (ca. 203~203.5 Ma, Fig. 9), with distributary channels and interdistributary bay deposits (Figs. 4 and 9). The coal accumulation was enhanced in a stable peat swamp of the interdistributary bay environment, and some thick, industry grade coal seams developed in the lower mudstone beds of Member V (e.g., upper part of Bed 9, Fig. 4).

Subsequently, the environment became disturbed again, as suggested by the mudstone breccia of the upper beds of Member V. The mudstone breccia composed of angular boulders suggest either an exceptional storm or even a tsunami event (Pole et al., 2018). Under this disturbed environment background, very few plant fossils could be preserved. Root clay and siderite concretions occurred in the upper beds of Member V, suggesting fluctuations of the lake level (Fig. 9). The disturbed environmental conditions extended throughout the upper Member V and the Member VI. The occurrence of both hummocky and swaley cross beddings in Member VI were proposed as strong evidence of more stormy conditions (Pole et al., 2018). The fine-grained and well-sorted quartz sandstone with wave-ripple marks of the Member VI may suggest a wave-dominated, near-shore environment.

Influenced by the lake transgression, a stable lakeshore and shallow lake environment developed prior to the Tr–J transition (Fig. 9). The depositional environment and facies evolution were mainly controlled by lake level changes. With the fall of lake level, a peat swamp environment occurred and the Xuanhan area became the coal depocenter, with industry grade, thick coal seams accumulated related to the stable environment conditions of Member VII (Fig. 2-F).

5.2 Palaeoclimate implications and ecological response

Species diversity, community composition and dominant taxa of the fossil assemblages can allow for inferences on palaeoclimate variations and palaeo-ecosystem stability (McElwain et al., 2007). Furthermore, syntheses of the sedimentary systems, community succession and major geological events contribute to better understanding of the ecological response of the Xujiahe Flora to the end-Triassic mass extinction and associated climatic and environmental change at that time (Fig. 9).

The observed water-level transgression across the wider depositional environment resulted in the formation of a transitional environment, which provided the initial habitats for the rise of the Xujiahe Flora in the latest Norian (ca. 207~207.2 Ma, Fig. 9). The thriving coastal hydrophyte community (CHC) of the Member I marked the origin of the Xujiahe Flora in the latest Norian in the

Xuanhan area. Both the community composition and the dominant taxa indicate hot and humid climatic conditions (Lu et al., 2019).

Subsequently, an environmentally disturbed floodplain developed during the uplift of the Qinling orogen across the Norian–Rhaetian transition (ca. 205~207 Ma, Fig. 9), terminating the favorable habitats for terrestrial plant ecosystems as described above. Locally, only the sphenopsid *Neocalamites* survived and became the dominant element, but *Podozamites* leaves, mainly transported and buried in the banks of lake or marshes, indicate a nearshore hydrophyte ecosystem as preserved in Member II (Huang and Lu, 1992). The occurrence of the fossil wood *Xenoxylon guangyuanensis* in the neighboring region of this basin was notable (Tian et al., 2016). Previously evidence suggests that the genus *Xenoxylon* was mainly distributed in the high latitude regions and reflecting cool and/or wet climate conditions, the southernmost occurrences of *Xenoxylon* in regions otherwise under warm or dry paleoclimates might indicate global colder/wetter climatic snaps (Philippe and Thévenard, 1996; Philippe et al., 2009). Therefore, the *X. guangyuanensis* would suggest a climatic cooling event linked to the development of the Late Triassic megamonsoon (Tian et al., 2016), influencing the evolution of gymnosperms.

Nearshore peat swamps developed as a result of lake level rise (Fig. 9). A community dominated by ferns, cycads and horsetails was thriving for a short period of time during the early Rhaetian (ca. 204.5 Ma, Fig. 9). The occurrence of ginkgophyte fossils (*Stachyopitys*) indicate that the climate was not as hot as during the latest Norian, and the delta plain wetlands community (DWC) of Member III represented the rise of the Xujiahe Flora in the early Rhaetian (Lu et al., 2019).

The second gap, induced by the Anxian Movement, influenced the floral communities again (Member VI, Fig. 9), coeval with the uplift of Longmenshan mountain-range towards the southwest, blocking the warm, moist water flow from the Tethys Ocean, deeply re-shaping local humidity patterns and the regional climate (Lu, 2019).

In the Middle Rhaetian (ca. 203~203.5 Ma, Beds 9 and 11 of Member V, Fig. 9), ferns and cycads were still dominant (Figs. 6 and 8). The ratio of fern spores was even as high as 71.78%, whereas the conifer pollen is only 15.34% (sample QLX-10 of Bed 9, Member V; Fig. 8). Both the macro- and micro- fossils indicate a swamp wetlands community (SWC) of the lower beds of Member V, growing under a warm and humid climate. Although the conifers and ginkgophytes showed higher diversity than the CHC of Member I and the DWC of Member III (Fig. 6), the abundance was still low and they were not the dominant groups.

Community destabilization marked the third gap of the floral succession at the study locality, suggesting a precursor interval of environmental stress in the late Rhaetian (ca. 202~203 Ma, Fig. 9). The mudstone breccia of Member V and the occurrence of both hummocky and swaley cross beddings in Member VI recorded the stormy conditions (Pole et al., 2018). The detrital charcoal fragments and inertinite recovered from the samples of the Xujiahe Formation also indicate a disturbed environment marked by intensive wildfire events (Pole et al., 2018; Lu, 2019). This ecosystem disturbance is also indicated by a series of discrete spikes in sulfide content and changes in planktonic community composition in the Panthalassic Ocean prior to the Tr–J boundary (Schoepfer et al., 2022).

Until the terminal Rhaetian, a stable nearshore environment became the refuge of the Xujiahe Flora in the Xuanhan area. Not only did the favorable habitats permitted the prosperity of the ferns, but also, it contributed to the diversification of conifers and ginkgophytes. Unlike the communities of the underlying members, the transitional community succession (TCs) of the Member VII showed an upward non-uniformity (Figs. 6, 8 and 9). Some hydrophyte taxa (e.g., *Neocalamites*) were preserved in the lowermost mudstone layers (TC-1), co-existing with some bivalve fossils (Ye et al., 1986; Huang and Lu, 1992). With the drop of the lake level, the shallow lake retreated and the lake shoreline changed, with the lakeshore subfacies becoming dominant. Within the lakeshore swamp microfacies, the wetland taxa became dominant in the Xuanhan area (TC-2). With the continuous drop of the lake level, the river dynamics became the main sedimentary feature and the flood plain expanded. Both the highland and the wetland taxa (i.e., conifers, ferns) were diverse and abundant in the middle mudstone layers of the Member VII (TC-2, 3). The bivalve fossils demonstrate the rise of lake level in the topmost bed of Member VII (Ye et al., 1986; Huang and Lu, 1992), with only a low-diversity floral community dominated by some upland xerophytic taxa (TC-4). The floral associations of the Member VII show an ecological collapse to the end of the Rhaetian (ca. 201.5~202 Ma, Fig. 9).

It is notable that the turnover from TC-2 to TC-3 and the ecological collapse is correlated with mercury enrichment prior to the Tr–J transition, as a CAMP global influence (Shen et al., 2022) (Fig. 9). Previous studies proposed that the Central Atlantic Magmatic Province (CAMP) volcanism have increased the frequency and scale of extreme climatic events (McElwain et al., 1999, 2007; Belcher et al., 2010), so that the enormous ecological pressure ultimately destroyed the terrestrial flora and generally their ecosystems (McElwain et al., 1999, 2007; Steinthorsdottir et al., 2012; Mander et al., 2013; Lindström et al., 2017; Capriolo et al., 2020; Yager et al., 2021). Recently, wildfire events across the Tr–J interval were identified at the Qilixia Section and throughout the whole basin (Pole et al., 2018; Lu, 2019; Song et al., 2020). Moreover, a multiproxy analysis (including organic carbon isotopes, mercury (Hg) concentrations and isotopes, chemical index of alteration (CIA), and clay minerals) of the Xujiahe Formation, across the Tr–J interval at Qilixia Section was undertaken (Shen et al., 2022). The increasing CIA in association with Hg peaks was interpreted as results of reflecting the volcanism-induced intensification of continental chemical weathering, which were linked with the CAMP event (Shen et al., 2022). Therefore, the ecological collapse in the end of the Rhaetian in the Xuanhan area was suggested to be largely induced by the CAMP emplacement and its associated climatic effects.

6 Conclusions

1) The Upper Triassic Xujiahe Formation yields the best record of the major changes of palaeogeography, palaeoclimate and palaeoecology occurring in the Late Triassic of the northeastern Sichuan Basin, South China. The oscillating fluvial-lacustrine depositional system during the late Triassic, and the sedimentary evolution of the basin were mainly controlled by the Indosinian Movement and by the regression-transgression cycle.
2) Within an overall warm and humid climate during the Late Triassic in the Xuanhan area, some climatic variations occurred, inferred from differences in floral communities of each member. The cooling and drying fluctuations influenced the diversification of gymnosperms.
3) Four communities and three obvious gaps document the rise and demise of Xujiahe Flora throughout the Late Triassic in the northeast Sichuan Basin. The floral community successions were closely related to sedimentary processes and to climatic variations. An ecosystem destabilization occurred in the Xuanhan area over one million years prior to the Tr–J interval, followed by an ecological collapse occurring at the Tr–J interval.
4) The Xujiahe Flora always recovered from the interruptions induced by tectonic movement, and it ultimately collapsed under the extreme climatic events and ecological pressure induced by the CAMP event.

Conflict of Interest

The authors declare that the research was conducted in the absence of any commercial or financial relationships that could be construed as a potential conflict of interest.

Author Contributions

YW, MEP and NL designed the study. NL, YX, LL, HC, XX, MR, MEP, WMK and YW carried out the field works. NL, YX and LL performed the lab works. NL, YX, LL and YW wrote the draft. All authors contributed to the interpretation and revision of the manuscript.

Funding

This study is financially supported by the National Natural Science Foundation of China (42202020, 41972120 and 42072009), and the Programs from State Key Lab of Palaeobiology and Stratigraphy (20191103, 213112).

Acknowledgments

We would like to thank Prof. Yue Li from Nanjing Institute of Geology and Palaeontology, Chinese Academy of Sciences for the suggestions regarding the manuscript. We appreciate Dr. Mingsong Li from Peking University and Senior Engineer Shuna Xi from the No. 137 Geological Survey of the Sichuan Coalfield Geology Bureau for their kind assistance during fieldtrips.

References

Atkinson, J.W., Wignall, P.B., Morton, J.D., Aze, T., and Hautmann, M. (2019). Body size changes in bivalves of the family Limidae in the aftermath of the end-Triassic mass extinction: the Brobdingnag effect. Palaeontology 62(4), 561-582. doi: 10.1111/pala.12415.

Barash, M.S. (2015). Abiotic causes of the great mass extinction of marine biota at the Triassic-Jurassic boundary. Oceanology 55(3), 374-382. doi: 10.1134/s0001437015030017.

Barbacka, M., Pacyna, G., Kocsis, Á.T., Jarzynka, A., Ziaja, J., and Bodor, E. (2017). Changes in terrestrial floras at the Triassic-Jurassic Boundary in Europe. Palaeogeography, Palaeoclimatology, Palaeoecology 480, 80-93. doi: 10.1016/j.palaeo.2017.05.024.

Belcher, C.M., Mander, L., Rein, G., Jervis, F.X., Haworth, M., Hesselbo, S.P., et al. (2010). Increased fire activity at the Triassic/Jurassic boundary in Greenland due to climate-driven floral change. Nature Geoscience 3(6), 426-429. doi: 10.1038/ngeo871.

Benton, M.J. (1986). More than one event in the late Triassic mass extinction. Nature 321(6073), 857-861. doi: 10.1038/321857a0.

Benton, M.J. (1995). Diversification and extinction in the history of life. Science 268(5207), 52-58. doi: 10.1126/science.7701342.

Capriolo, M., Marzoli, A., Aradi, L.E., Callegaro, S., Dal Corso, J., Newton, R.J., et al. (2020). Deep CO_2 in the end-Triassic Central Atlantic Magmatic Province. Nature communications 11(1), 1670. doi: 10.1038/s41467-020-15325-6.

Cascales-Miňana, B., and Cleal, C.J. (2012). Plant fossil record and survival analyses. Lethaia 45(1), 71-82. doi: 10.1111/j.1502-3931.2011.00262.x.

Cleveland, D.M., Nordt, L.C., Dworkin, S.I., and Atchley, S.C. (2008). Pedogenic carbonate isotopes as evidence for extreme climatic events preceding the Triassic-Jurassic boundary: Implications for the biotic crisis? Geological Society of America Bulletin 120(11-12), 1408-1415. doi: 10.1130/b26332.1.

Deng, K. (1996). "Formation and development of Sichuan Basin," in Sichuan Basin Formation and Development, ed. Z. Guo. (Beijing: Geilogical Publishing House), 113-138.

Fowell, S.J., and Olsen, P.E. (1993). Time calibration of Triassic/Jurassic microfloral turnover, eastern North America. Tectonophysics 222(3-4), 361-369. doi: 10.1016/0040-1951(93)90359-r.

Götz, A.E., Ruckwied, K., Pálfy, J., and Haas, J. (2009). Palynological evidence of synchronous changes within the terrestrial and marine realm at the Triassic/Jurassic boundary (Csővár section, Hungary). Review of Palaeobotany and Palynology 156(3-4), 401-409. doi: 10.1016/j.revpalbo.2009.04.002.

Gou, Z. (1998). The Bivalve Faunas from the Upper Triassic Xujiahe Formation in the Sichuan Basin. Sedimentary Facies and Palaeogeography 18(2), 20-29.

Hallam, A. (2002). How catastrophic was the end-Triassic mass extinction? Lethaia 35(2), 147-157. doi: 10.1080/00241160232018406.

He, L. (2014). Permian to Late Triassic evolution of the Longmen Shan Foreland Basin (Western Sichuan): Model results from both the lithospheric extension and flexure. Journal of Asian Earth Sciences 93, 49-59. doi: 10.1016/j.jseaes.2014.07.007.

He, T., Dal Corso, J., Newton, R.J., Wignall, P.B., Mills, B.J.W., Todaro, S., et al. (2020). An enormous sulfur isotope excursion indicates marine anoxia during the end-Triassic mass extinction. Science Advances 6(37), eabb6704. doi: 10.1126/sciadv.abb6704.

Hesselbo, S.P., McRoberts, C.A., and Pálfy, J. (2007). Triassic–Jurassic boundary events: Problems, progress, possibilities. Palaeogeography, Palaeoclimatology, Palaeoecology 244(1), 1-10. doi: 10.1016/j.palaeo.2006.06.020.

Hesselbo, S.P., Robinson, S.A., Surlyk, F., and Piasecki, S. (2002). Terrestrial and marine extinction at the Triassic-Jurassic boundary synchronized with major carbon-cycle perturbation: A link to initiation of massive volcanism? Geology 30(3), 251-254. doi: 10.1130/0091-7613(2002)030<0251:Tameat>2.0.Co;2.

Huang, Q. (1995). Palaeoclimate and coal-forming characteristics of the Late Triassic Xujiahe Stage in northern Sichuan. Geological Review 41(1), 92-99.

Huang, Q., and Lu, S. (1992). The Primary Studies on the Palaeoecology of the Late Triassic Xujiahe Flora in Eastern Sichuan. Earth Science-Journal of China University of Geosciences 17(3), 329-335.

Korte, C., Ruhl, M., Ullmann, C.V., and Hesselbo, S.P. (2019). "Chemostratigraphy Across the Triassic–Jurassic Boundary," in Chemostratigraphy Across Major Chronological Boundaries, eds. A.N. Sial, C. Gaucher, M. Ramkumar & V.P. Ferreira. (US: American Geophysical Union), 185-210.

Kürschner, W.M., Bonis, N.R., and Krystyn, L. (2007). Carbon-isotope stratigraphy and palynostratigraphy of the Triassic–Jurassic transition in the Tiefengraben section — Northern Calcareous Alps (Austria). Palaeogeography, Palaeoclimatology, Palaeoecology 244(1), 257-280. doi: 10.1016/j.palaeo.2006.06.031.

Kustatscher, E., Ash, S.R., Karasev, E., Pott, C., Vajda, V., Yu, J., et al. (2018). "Flora of the Late Triassic," in The Late Triassic World, ed. H. Tanner Lawrence. Springer), 545-622.

Li, J., Huang, C., Wen, X., and Zhang, M. (2021). Mesozoic paleoclimate reconstruction in Sichuan Basin, China: Evidence from deep-time paleosols. Acta Sedimentologica Sinica 39(5), 1157-1170. doi: 10.14027/j.issn.1000-0550.2020.058.

Li, L., Wang, Y., Kürschner, W.M., Ruhl, M., and Vajda, V. (2020). Palaeovegetation and palaeoclimate changes across the Triassic–Jurassic transition in the Sichuan Basin, China. Palaeogeography, Palaeoclimatology, Palaeoecology 556, 109891. doi: 10.1016/j.palaeo.2020.109891.

Li, L., Wang, Y., Liu, Z., Zhou, N., and Wang, Y. (2016). Late Triassic palaeoclimate and palaeoecosystem variations inferred by palynological record in the northeastern Sichuan Basin, China. PalZ 90(2), 327-348. doi: 10.1007/s12542-016-0309-5.

Li, L., Wang, Y., Vajda, V., and Liu, Z. (2018). Late Triassic ecosystem variations inferred by palynological records from Hechuan, southern Sichuan Basin, China. Geological Magazine 155(8), 1793-1810. doi: 10.1017/s0016756817000735.

Li, M., Zhang, Y., Huang, C., Ogg, J., Hinnov, L., Wang, Y., et al. (2017). Astronomical tuning and magnetostratigraphy of the Upper Triassic Xujiahe Formation of South China and Newark

Supergroup of North America: Implications for the Late Triassic time scale. Earth and Planetary Science Letters 475, 207-223. doi: 10.1016/j.epsl.2017.07.015.

Lindström S., van de Schootbrugge B., Hansen K.H., Pedersen, G.K., Alsen, P., Thibault, N., Dybkjær, K., Bjerrum, C.J., Nielsen, L.H. (2017). A new correlation of Triassic–Jurassic boundary successions in NW Europe, Nevada and Peru, and the Central Atlantic Magmatic Province: A time-line for the end-Triassic mass extinction. Palaeogeography, Palaeoclimatology, Palaeoecology. 478: 80-102. doi.org/10.1016/j.palaeo.2016.12.025.

Liu, S., Yang, Y., Deng, B., Zhong, Y., Wen, L., Sun, W., et al. (2021). Tectonic evolution of the Sichuan Basin, Southwest China. Earth-Science Reviews 213. doi: 10.1016/j.earscirev.2020.103470.

Liu, Z., Li, L., and Wang, Y. (2015). Late Triassic spore-pollen assemblage from Xuanhan of Sichuan, China. Acta Micropalaeontologica Sinica 32(1), 43-62. doi: 10.16087/j.cnki.1000-0674.20150407.006.

Lee, P.-C. (1964). Fossil plants from the Hsuchiaho Series od Kwangyüan, northern Szechuan. Memoirs of Institute of Geology and Palaeontology, Academia Sinica (3), 101-178.

Lu, N. (2019). Changes in sedimentary environment and terrestrial paleoecology across the Triassic-Jurassic transition in eastern Sichuan Basin. doctoral thesis, University of Science and Technology of China.

Lu, N., Li, Y., Wang, Y., Xu, Y., and Zhou, N. (2021). Fossil dipterid fern *Thaumatopteris* in China: new insights of systematics, diversity and tempo-spatial distribution patterns. Historical Biology 33(10), 2316-2329. doi: 10.1080/08912963.2020.1791106.

Lu, N., Wang, Y., Popa, M.E., Xie, X., Li, L., Xi, S., et al. (2019). Sedimentological and paleoecological aspects of the Norian–Rhaetian transition (Late Triassic) in the Xuanhan area of the Sichuan Basin, Southwest China. Palaeoworld 28(3), 334-345. doi: 10.1016/j.palwor.2019.04.006.

Lu, N., Xie, X., Wang, Y., and Li, L. (2015). The Analysis of Sedimentary Environmental Evolution of the T3x/T2l Boundary Transition in Qilixia of Xuanhan, Sichuan. Acta Sedimentologica Sinica 33(6), 1149-1158.

Lucas, S.G., and Tanner, L.H. (2015). End-Triassic nonmarine biotic events. Journal of Palaeogeography 4(4), 331-348. doi: 10.1016/j.jop.2015.08.010.

Lucas, S.G., and Tanner, L.H. (2018). "The Missing Mass Extinction at the Triassic-Jurassic Boundary," in The Late Triassic World, ed. H. Tanner Lawrence. Springer), 721-785.

Mander, L., Kürschner, W.M., and McElwain, J.C. (2013). Palynostratigraphy and vegetation history of the Triassic–Jurassic transition in East Greenland. Journal of the Geological Society 170(1), 37-46. doi: 10.1144/jgs2012-018.

Marzoli, A., Bertrand, H., Knight, K.B., Cirilli, S., Buratti, N., Vérati, C., et al. (2004). Synchrony of the Central Atlantic magmatic province and the Triassic-Jurassic boundary climatic and biotic crisis. Geology 32(11). doi: 10.1130/g20652.1.

McElwain, J.C., Beerling, D.J., and Woodward, F.I. (1999). Fossil plants and global warming at the Triassic-Jurassic boundary. Science 285(5432), 1386-1390. doi: 10.1126/science.285.5432.1386.

McElwain, J.C., Popa, M.E., Hesselbo, S.P., Haworth, M., and Surlyk, F. (2007). Macroecological responses of terrestrial vegetation to climatic and atmospheric change across the Triassic/Jurassic boundary in East Greenland. Paleobiology 33(4), 547-573. doi: 10.1666/06026.1.

McElwain, J.C., and Punyasena, S.W. (2007). Mass extinction events and the plant fossil record. Trends in Ecology and Evolution 22(10), 548-557. doi: 10.1016/j.tree.2007.09.003.

Mihca, R., Bonis N.R., Reichart, G.-J., Damsté J.S.S., and Kürschner W.M., (2011). Atmospheric Carbon Injection Linked to End-Triassic Mass Extinction. Science 333(6041), 430-434.

Ruhl, M., Hesselbo, S.P., Al-Suwaidi, A., Jenkyns, H.C., Damborenea, S.E., Manceñido, M.O., Storm, M., Mather, T.A., and Riccardi, A.C. (2020). On the onset of Central Atlantic Magmatic Province (CAMP) volcanism and environmental and carbon-cycle change at the Triassic–Jurassic transition (Neuquén Basin, Argentina). Earth-Science Reviews 208, 103229. doi.org/10.1016/j.earscirev.2020.103229.

Michalík, J., Lintnerová, O., Gaździcki, A., and Soták, J. (2007). Record of environmental changes in the Triassic–Jurassic boundary interval in the Zliechov Basin, Western Carpathians. Palaeogeography, Palaeoclimatology, Palaeoecology 244(1), 71-88. doi: 10.1016/j.palaeo.2006.06.024.

Olsen, P.E., Kent, D.V., Sues, H.D., Koeberl, C., Huber, H., Montanari, A., et al. (2002). Ascent of dinosaurs linked to an iridium anomaly at the Triassic-Jurassic boundary. Science 296(5571), 1305-1307. doi: 10.1126/science.1065522.

Parrish, J.T., and Peterson, F. (1988). Wind directions predicted from global circulation models and wind directions determined from eolian sandstones of the western United States-a comparison. Sedimentary Geology 56(1-4), 261–282.

Percival, L.M.E., Ruhl, M., Hesselbo, S.P., Jenkyns, H.C., Mather, T.A., and Whiteside, J.H. (2017). Mercury evidence for pulsed volcanism during the end-Triassic mass extinction. Proceedings of the National Academy of Sciences 114(30), 7929. doi: 10.1073/pnas.1705378114.

Philippe, M., Thévenard, F. (1996). Repartition and palaeoecology of the Mesozoic wood genus Xenoxylon: palaeoclimatological implications for the Jurassic of Western Europe. Review of Palaeobotany and Palynology 91(1-4), 353–370. doi: 10.1016/0034-6667(95)00067-4

Philippe, M., Jiang, H.E., Kim, K., Oh, C., Gromyko, D., Harland, M., Paik, I.S., Thévenard, F. (2009). Structure and diversity of the Mesozoic wood genus Xenoxylon in Far East Asia: implications for terrestrial palaeoclimates. Lethaia 42(4), 393–406. Doi: 10.1111/j.1502-3931.2009.00160.x.

Pole, M., Wang, Y., Dong, C., Xie, X., Tian, N., Li, L., et al. (2018). Fires and storms—a Triassic–Jurassic transition section in the Sichuan Basin, China. Palaeobiodiversity and Palaeoenvironments 98(1), 29-47. doi: 10.1007/s12549-017-0315-y.

Raup, D.M., and Sepkoski, J.J. (1982). Mass extinctions in the marine fossil record. Science 215(4539), 1501-1503. doi: 10.1126/science.215.4539.1501.

Schoepfer, S.D., Shen, J., Sano, H., and Algeo, T.J. (2022). Onset of environmental disturbances in the Panthalassic Ocean over one million years prior to the Triassic-Jurassic boundary mass extinction. Earth-Science Reviews 224**,** 103870.

Sepkoski, J.J. (1981). A factor analytic description of the Phanerozoic marine fossil record. Paleobiology 7(1), 36-53.

Shen, J., Yin, R., Zhang, S., Algeo, T.J., Bottjer, D.J., Yu, J., Xu, G., Penman, D., Wang, Y., Li, L., Shi, X., Planavsky, N.J., Feng, Q., and Xie, S. (2022). Intensified continental chemical weathering and carbon-cycle perturbations linked to volcanism during the Triassic–Jurassic transition. Nature Communications 13**,** 299. doi: 10.1038/s41467-022-27965-x.

Song, Y., Algeo, T.J., Wu, W., Luo, G., Li, L., Wang, Y., et al. (2020). Distribution of pyrolytic PAHs across the Triassic-Jurassic boundary in the Sichuan Basin, southwestern China:

Evidence of wildfire outside the Central Atlantic Magmatic Province. Earth-Science Reviews 201, 102970. doi: 10.1016/j.earscirev.2019.102970.

Stanley, G.D., Jr., Shepherd, H.M.E., and Robinson, A.J. (2018). Paleoecological Response of Corals to the End-Triassic Mass Extinction: An Integrational Analysis. Journal of Earth Science 29(4), 879-885. doi: 10.1007/s12583-018-0793-5.

Steinthorsdottir, M., Woodward, F.I., Surlyk, F., and McElwain, J.C. (2012). Deep-time evidence of a link between elevated CO_2 concentrations and perturbations in the hydrological cycle via drop in plant transpiration. Geology 40(9), 815-818. doi: 10.1130/g33334.1.

Sun, G., Meng, F., Qian, L., and Ouyang, S. (1995). "Triassic floras," in Fossil floras of China through the geological ages, ed. X. Li. (Guangzhou, China: Guangdong Science and Technology Press), 305-342.

Tian, N., Wang, Y., Philippe, M., Li, L., Xie, X., and Jiang, Z. (2016). New record of fossil wood *Xenoxylon* from the Late Triassic in the Sichuan Basin, southern China and its paleoclimatic implications. Palaeogeography, Palaeoclimatology, Palaeoecology 464, 65-75. doi: 10.1016/j.palaeo.2016.02.006.

Tomašových, A., and Siblík, M. (2007). Evaluating compositional turnover of brachiopod communities during the end-Triassic mass extinction (Northern Calcareous Alps): Removal of dominant groups, recovery and community reassembly. Palaeogeography, Palaeoclimatology, Palaeoecology 244(1), 170-200. doi: 10.1016/j.palaeo.2006.06.028.

Van de Schootbrugge, B., Quan, T.M., Lindström, S., Püttmann, W., Heunisch, C., Pross, J., et al. (2009). Floral changes across the Triassic/Jurassic boundary linked to flood basalt volcanism. Nature Geoscience 2(8), 589-594. doi: 10.1038/ngeo577.

Wang, C., Zheng, R., Li, S., Li, S., Li, G., et al. (2017). Stratigraphic Subdivision and Correlation of the Upper Triassic Xujiahe Formation, Eastern Sichuan Basin: A Case Study of the Woxinshuang Area. Journal of Stratigraphy 41(1), 94-102.

Wang, J. (1990). Anxian tectonic movement. Oil & Gas Geology 11(3), 223-234.

Wang, J. (2003). Recognition on the main episode of Indo-China Movement in the Longmen Moutains. Acta Geologica Sichuan 23(2), 65-69.

Wang, Y., Fu, B., Xie, X., Huang, Q., Li, K., Li, G., et al. (2010). The Terrestrial Triassic and Jurassic Systems in the Sichuan Basin, China. Hefei, China: University of Sicence and Technology of China Press.

Wang, Y., Li, L.Q., Guignard, G., Dilcher, D.L., Xie, X., Tian, N., et al. (2015). Fertile structures with in situ spores of a dipterid fern from the Triassic in southern China. Journal of Plant Research 128(3), 445-457. doi: 10.1007/s10265-015-0708-9.

Whiteside, J.H., Olsen, P.E., Eglinton, T., Brookfield, M.E., and Sambrotto, R.N. (2010). Compound-specific carbon isotopes from Earth's largest flood basalt eruptions directly linked to the end-Triassic mass extinction. Proc Natl Acad Sci U S A 107(15), 6721-6725. doi: 10.1073/pnas.1001706107.

Williford, K.H., Foriel, J., Ward, P.D., and Steig, E.J. (2009). Major perturbation in sulfur cycling at the Triassic-Jurassic boundary. Geology 37(9), 835-838. doi: 10.1130/g30054a.1.

Wotzlaw, J.F., Guex, J., Bartolini, A., Gallet, Y., Krystyn, L., McRoberts, C.A., et al. (2014). Towards accurate numerical calibration of the Late Triassic: High-precision U-Pb geochronology constraints on the duration of the Rhaetian. Geology 42(7), 571-574. doi: 10.1130/g35612.1.

Wu, S. (1983). “On the Late Triassic and Early-Middle Jurassic Floras and Their Distributions in China," in Palaeobiogeographic Provinces of China, ed. E.C.o.F.T.o.P.B. Series. (Beijing: Science Press), 121-130.

Wu, S. (1999). Upper Triassic plants from Sichuan. Bulletin of Nanjing Institute of Geology and Palaeontology, Academia Sinica (14), 1-69.

Xu, Y., Popa, M.E., Zhang, T., Lu, N., Zeng, J., Zhang, X., et al. (2021). Re-appraisal of *Anthrophyopsis* (Gymnospermae): New material from China and global fossil records. Review of Palaeobotany and Palynology 292. doi: 10.1016/j.revpalbo.2021.104475.

Yager, J.A., West, A.J., Thibodeau, A.M., Corsetti, F.A., Rigo, M., Berelson, W.M., Bottjer, D.J., Greene, S.E., Ibarra, Y., Jadoul, F., Ritterbush, K.A., Rollins, N., Rosas, S., Di Stefano, P., Sulca, D., Todaro, S., Wynn, P., Zimmermann, L., Bergquist, B.A. (2021). Mercury contents and isotope ratios from diverse depositional environments across the Triassic–Jurassic Boundary: Towards a more robust mercury proxy for large igneous province magmatism. Earth-Science Reviews 223, 103775. doi.org/10.1016/j.earscirev.2021.103775.

Ye, M., Liu, X., Huang, G., Chen, L., Peng, S., et al. (1986). Late Triassic and Early-Middle Jurassic Fossil Plants from Northeastern Sichuan. Hefei: Anhui Science and Technology Publishing House.

Zhong, D. (1998). Paleotethysides of the western Guizhou-Sichuan region. Beijing: Science Press

Zhu, M., Chen, H., Zhou, J., and Yang, S. (2017). Provenance change from the Middle to Late Triassic of the southwestern Sichuan basin, Southwest China: Constraints from the sedimentary record and its tectonic significance. Tectonophysics 700-701, 92-107. doi: 10.1016/j.tecto.2017.02.006.

Figure Captions

Fig. 1 Maps showing the location of the Qilixia Section, NE Sichuan Basin, China.

A. The palaeogeographic location of Sichuan Basin during the Rhaetian (Base map after Metcalfe, 2011); **B**. The location of the Qilixia Section, NE Sichuan Basin; **C**. Simplified geological map of the Qilixia Section and surrounding region (after Sichuan Bureau of Geology, 1980).

Fig. 2 Stratigraphic boundaries and lithologies of the Xujiahe Formation at the Qilixia Section.

A. The lithological boundary between the Upper Triassic Xujiahe Formation and the Middle Triassic Leikoupo Formation; **B**. The lithological boundary between the Lower Jurassic Zhenzhuchong Formation and the Upper Triassic Xujiahe Formation; **C**. The massive sandstone bed of Member II; **D**. The sandstone bed with carbonized branches of Member IV; **E**. The mudstone bed with siderite concretions of Member I; **F**. The fossils bearing layers and coal seam of Member VII; **G**. The conglomerate layer of Member II; **H**. The conglomerate layer with tree trunks of Member II.

Fig. 3 Sedimentary structures of the Xujiahe Formation at the Qilixia Section.

A. The sandstone bed with conglomerate lens and erosion surface of Member II; **B**. The parallel beddings of Member IV; **C**. The cross beddings of Member VI; **D**. The climbing ripples of Member IV; **E**. The wave-ripple marks of Member VI; **F**. The load casts of Member II; **G**. The mud cracks of Member I; **H**. The *Skolithos* burrows of Member III (after Pole et al., 2018).

Fig. 4 Detailed log showing the lithology, sedimentary structures, fossil preservation and sedimentary sequences of the Xujiahe Formation at the Qilixia Section.

Fig. 5 Representatives of the Xujiahe Flora collected from the Qilixia Section.

A. *Radicites* sp., Member I, QLX2014103; **B**. *Neocalamites* sp., Member II; **C**. *Pterophyllum angustum* (Braun) Gothan, Member V, QLX2014163; **D**. *Cladophlebis raciborskii* Zeiller, Member V, QLX2014146; **E**. 01, *Ixostrobus* sp.; 02, *Podozamites* sp., Member V, QLX2014159; **F**. *Cladophlebis* sp., Member V, QLX2014170; **G**. *Baiera elegans* Oishi, QLX2014350; **H.** *Ginkgoites sibiricus* (Heer) Seward, Member VII, QLX-2105-15U-542; **I.** *Cladophlebis* sp., Member VII, QLX2014399; **J.** *Dictyophyllum nathorsti* Zeiller, Member VII, QLX-2105-15U-680a. (A, C-J, scale bar = 10 mm; B, scale bar = 50 mm; The plant fossils are showing in the stratigraphic order).

Fig. 6 Stratigraphic occurrences of the plant macrofossils and division of the floral communities of the Late Triassic Xujiahe Flora.

*The division of the floral communities are based on the plant macrofossils and palynological data.

Fig. 7 Representative spore and pollen taxa recovered from the Xujiahe Formation at the Qilixia section.

A. *Sphagnumsporites clavus* (Balme, 1957) Huang, 2000, Member I, QLX-1-1; **B**. *Sphagnumsporites perforates* (Leschik) Liu, 1986, Member I, QLX-1-4; **C**. *Cibotiumspora robusta* Lu et Wang, 1983, Member I, QLX-1-1; **D**. *Dictyophyllidites harrisii* Couper, 1958, Member I, QLX-1-1; **E**. *Toroisporis minoris* (Nakoman) Sun et He, 1980, Member I, QLX-1-3; **F,** *Toroisporis minoris* (Nakoman) Sun et He, 1980, Member III, QLX-7-7; **G.** *Concavisporites toralis* (Leschik, 1955) Nilsson, 1958, Member I, QLX-1-3; **H.** *Cyathidites minor* Couper, 1953, Member I, QLX-1-4; **I.** *Osmundacidites granulata* (Mal.) Zhou, 1981, Member I, QLX-2-1; **J.** *Cyclogranisporites arenosus* Madler, 1964, Member III, QLX-8-2; **K.** *Angiopteridaspora denticulata* Chang, 1965, Member I, QLX-1-1; **L.** *Granulatisporites triconvexus* Staplin, 1960, Member I, QLX-1-4; **M.** *Osmundacidites wellmanii* Couper, 1953, Member III, QLX-9-2; **N.** *Planisporites dilucidus* Megregor, 1960, Member V, QLX-12-2; **O.** *Araucariacites australis* Cookson, 1947, Member I, QLX-1-3; **P.** *Alisporites parvus* De Jersey, 1962, Member VII, XHQL-89-5; **Q.** *Alisporites parvus* De Jersey, 1962, Member

VII, XHQL-91-1; **R.** *Vitreisporites pallidus* (Reissinger) Nilsson, 1958, Member II, XHQL-40-2; **S.** *Pinuspollenites divulgatus* (Bolkh.) Qu, 1980, Member VII, XHQL-91-1; **T.** *Pinuspollenites alatipollenites* (Rouse) Liu, 1982, Member VII, XHQL-91-1; **U.** *Piceites enodis* Bolkhovitina, 1956, Member II, QLX-2-1; **V.** *Quadraeculina anellaeformis* Maljavkina, 1949, Member VII, XHQL-89-1; **W.** *Podocarpidites unicus* (Bolkh.) Pocock, 1970, Member II, XHQL-40-1; **X.** *Cycadopites parvus* (Bolkh.) Pocock, 1970, Member I, QLX-1-1; **Y.** *Cycadopites follicularis* Wilson et Webster, 1946, Member II, XHQL-40-2; **Z.** *Cycadopites reticulata* (Nilsson) Arjang, 1975, Member VII, XHQL-91-1; **AA.** *Monosulcites granulatus* Couper 1960, Member VII, XHQL-91-1; **AB.** *Monosulcites minimus* Cookson, 1947, Member I, QLX-1-4; **AC.** *Monosulcites enormis* Jain, 1968, Member VII, XHQL-89-3. (scale bar = 20 μm)

Fig. 8 Stratigraphic occurrences and abundance diagram of major spore-pollen groups recovered from the Xujiahe Formation at the Qilixia section.

Fig. 9 Environmental oscillations and the ecological responses of the Xujiahe Formation at the Qilixia Section.

1). The 405-kyr eccentricity cycle and ages are from Li et al., 2017. **2)**. The initial- and main- carbon isotope excursions and mercury (Hg) isotope enrichment are from Shen et al., 2022.

Oscillations of a fluvial-lacustrine system and its ecological response prior to the end-Triassic: evidence from the eastern Tethys region

Ning Lu [1], Yongdong Wang [1,8*], Yuanyuan Xu [1,7], Liqin Li [1], Xiaoping Xie [4], Mihai Emilian Popa [2,3*], Hongyu Chen [1,7], Micha Ruhl [5], Wolfram Michael Kürschner [6]

[1]State Key Laboratory of Palaeobiology and Stratigraphy, Nanjing Institute of Geology and Palaeontology, Chinese Academy of Sciences, Nanjing 210008, China

[2]School of Geosciences and Technology, Southwest Petroleum University, Chengdu 610500, China

[3]University of Bucharest, Faculty of Geology and Geophysics, Doctoral School of Geology, Laboratory of Palaeontology, 1, N. Bălcescu Ave, Bucharest 010041, Romania

[4]School of Geography and Tourism, Qufu Normal University, Rizhao 276826, China

[5]Department of Geology, Trinity College Dublin, The University of Dublin, College Green, Dublin 2, Ireland

[6]Department of Geosciences, University of Oslo, N-0316 Oslo, Norway

[7]University of Chinese Academy of Sciences, Beijing 100049, China

[8]Nanjing College, University of Chinese Academy of Sciences, Nanjing 210006, China

*** Correspondence:**

Yongdong Wang: ydwang@nigpas.ac.cn

Mihai Emilian Popa: mihai@mepopa.com

Abstract

The end-Triassic mass extinction is considered as one of the "Big Five" extinction events in the Phanerozoic. However, whether the terrestrial ecosystem began to deteriorate or even collapse prior to the Triassic–Jurassic transition remains controversial. Compared with the documented data from the western Tethyan region, evidence from the eastern Tethyan realm is limited. We undertake a fitting analysis of the sedimentary system, floral community successions and major geological events of the Xujiahe Formation as reflected by the Qilixia Section, Xuanhan area, northeast Sichuan Basin, China. Our results reveal an oscillating fluvial-lacustrine depositional system during the Late Triassic, with the dominant sedimentary processes mainly controlled by the Indosinian Movement. Beside the sedimentary influence on the Xujiahe Flora, climate changes played a more important role. Fluctuating conditions to cooler and dryer climates at this time promoted diversification of gymnosperms under an overall warm and humid climate setting in the Late Triassic in the Xuanhan area. Superimposed on this oscillating long-term climate state, ecosystem destabilization occurred over one million years prior to the Tr–J interval in the Xuanhan study-area, possibly in response to the intensified storm and wildfire activity and the following environmental changes. Although the Xujiahe Flora always recover from the interruption of the tectonic movement, it ultimately collapsed under extreme climatic events and ecological pressures induced by the Late Triassic CAMP event.

Keywords: sedimentary oscillations, floral community succession, Central Atlantic Magmatic Province, end-Triassic mass extinction, Sichuan Basin.

1 Introduction

The Triassic-Jurassic transition (Tr–J, 201.36 ± 0.17 Ma, Wotzlaw et al., 2014) is marked by the end-Triassic mass extinction, one of the "Big Five" extinction events of the Phanerozoic (Sepkoski, 1981; Raup and Sepkoski, 1982; Benton, 1995). The biotic turnover, ecological crisis and environmental background across the Tr–J transition have drawn significant attention over the last decades (Hesselbo et al., 2007; Barash, 2015). The impact of the end-Triassic mass extinction on marine organisms has been extensively documented (e.g., radiolarians, Hallam, 2002; foraminifera, Michalík et al., 2007; ammonites and brachiopods, Tomašových and Siblík, 2007; corals and calcisponges, Stanley et al., 2018; bivalves, Atkinson et al., 2019). Bio- and chemo-stratigraphic data and stratigraphic correlations of sea-level changes, ocean acidification and release of greenhouse gases (e.g., CO_2, CH_4) suggest this event to be triggered by the breakup of Pangea and particularly by the eruptions of the Central Atlantic Magmatic Province (CAMP) at that time (Marzoli et al., 2004; Van de Schootbrugge et al., 2009; Whiteside et al., 2010; Ruhl et al., 2011, 2020; Percival et al., 2017; Capriolo et al., 2020; He et al., 2020). Extreme climatic events caused by significant global warming led to habitat and ecosystem disruption and destruction, with palynological and geochemical data suggesting this to have occurred simultaneously in the terrestrial and marine realms (McElwain et al., 1999; Hesselbo et al., 2002; Cleveland et al., 2008; Götz et al., 2009; Williford et al., 2009; Korte et al., 2019). However, the extinction patterns across this event remain controversial, with some suggestions for multiple extinction events throughout the Late Triassic instead of a single mass extinction at the end of the Late Triassic (Benton, 1986; Hallam, 2002; Lucas and Tanner, 2015, 2018). Considerable controversy derives from the response of terrestrial vegetation to these events. Studies of the plant taxonomic records from Greenland, North America, Europe and Gondwana revealed a significant floral turnover at species and community levels (Fowell and Olsen, 1993; McElwain et al., 1999; Olsen et al., 2002; McElwain and Punysasena, 2007; Küerschner et al., 2007; Belcher et al., 2010; Kustatscher et al., 2018). Other works considered that plant community changes across the Tr–J transition were linked to gradual and adaptive ecological reorganization related to long-term environmental variations, suggesting terrestrial plant changes to be local turnovers rather than associated with a mass extinction (Cascales-Miňana and Cleal, 2012; Barbacka et al. 2017; Lucas and Tanner, 2018; Zhou et al., 2021). As most studies on the end-Triassic mass extinction were carried out in the western Tethyan realm, especially in Europe and North America, critical insight on global changes, including as recorded in the eastern Tethyan realm is largely missing.

Terrestrial Tr–J transition sequences are well developed in the Sichuan Basin, southwestern China, representing the most expanded Tr–J strata in the eastern Tethyan realm (Wang et al., 2010). Fundamental studies on regional geology, stratigraphy and palaeontology were previously conducted (Wang et al., 2010), showing abundant yields of diverse plant fossils, represented by the Xujiahe Flora, in the Upper Triassic sequences of the Sichuan Basin (Ye et al., 1986; Huang, 1995; Wang et al., 2010). The Xujiahe Flora has been suggested to be flourishing under a tropical-subtropical hot and humid climatic conditions (Lee, 1964; Ye et al., 1986; Wu, 1983; Sun, 1995). In recent years, studies on systematic palaeobotany (Wang et al., 2015; Lu et al., 2021; Xu et al., 2021), palynology (Liu et al., 2015; Li et al., 2016, 2018), as well as sedimentology and geochemistry (Zhu et al., 2017; Pole et al., 2018; Lu et al., 2019; Shen et al., 2022) were conducted for these Upper Triassic sequences of the Sichuan Basin, showing notable temporal variations in climate at that time (Tian et al., 2016; Lu et al., 2019; Li et al., 2020; Li et al., 2021). The environmental evolution during the Late Triassic in the northeastern Sichuan Basin is as of yet poorly understood, it is critical to provide insight on the level of ecosystem stability, deterioration and/or collapse prior to the Tr–J transition in this region.

Here, we investigate the sedimentary succession and sedimentary features of the Upper Triassic sequences in the northeastern Sichuan Basin, with the emphasis on the significance of the macro- and micro-floral records related to their depositional context. We aim to reveal the environmental/climatic oscillations and ecological responses during the Rhaetian (Late Triassic) in the northeastern Sichuan Basin, next to discussion on the wider stability of terrestrial ecosystem prior to the Tr–J transition.

2 Geological Settings

The Sichuan Basin occurred on the northern frame of the eastern Tethyan realm (Fig. 1-A). This basin is one of the largest sedimentary basins in southwestern China, covering the eastern Sichuan Province and the majority of Chongqing City (Fig. 1-B). Its tectonic evolution can be divided into three stages: basement formation, craton basin and foreland basin (Wang et al., 2010). The igneous basement of the Sichuan Basin is Meso-Neoproterozoic in age. The sedimentary cover of the Sichuan Basin recorded a stable craton development stage, reflected by a set of shallow platform carbonate deposits. When the South China Block, the North China Block and the Songpan-Ganzi Terrane collided during the Late Triassic, the Sichuan foreland basin was formed, and the depositional environment changed from marine to terrestrial (Wang et al., 2010). During this time interval, both the end-Triassic mass extinction and the long-term formation of the Sichuan Basin were accurately, and continuously recorded in the Upper Triassic deposits.

The Upper Triassic sequences of the Sichuan Basin are represented by the Xujiahe Formation, a succession of clastic rocks with abundant coal and gas resources (Wang et al., 2010). The formation is widely distributed and well outcropped in the eastern and northeastern margins of the basin. The Qilixia Section is one of the key and well-known Upper Triassic-Lower Jurassic sections in this area, occurring close to Qili town in Xuanhan County, Dazhou City (Figs. 1-B, C). The Xujiahe Formation is about 520 m thick, outcropping along the road from Xuanhan to Kaijiang counties. The Xujiahe Formation unconformably overlies the Middle Triassic Leikoupo Formation and it is conformably overlain by the Lower Jurassic Zhenzhuchong Formation. The Xujiahe Formation is divided into seven members (Members I–VII) with distinct lithological boundaries between each member (Wang et al., 2010). Previous palaeobotanical and palynological data suggest that the Xujiahe Formation is

Norian to Rhaetian in age (Ye et al., 1986; Li et al., 2016, 2018, 2020). The combined cyclo- and magneto-stratigraphic record for this section and formation demonstrate that the age of the Xujiahe Formation spans from the latest Norian to the Rhaetian, i.e., from 207.2 Ma to 201.3 Ma (Li et al., 2017).

(Fig. 1 is approximately here)

3 Material and Methods

The Qilixia Section was here studied and sampled for sedimentological investigations. Facies analyses were conducted according to precise sequence data and sedimentary features (Figs. 2-4).

Published plant macrofossils of the Xujiahe Formation at the Qilixia Section were compiled and analyzed, revealing their ecology (Ye et al., 1986; Wu, 1999; Wang et al., 2010; Lu, 2019), and new plant specimens were collected and supplemented to the previously existing dataset, next to sporomorph data (Li et al., 2016, 2020; Lu et al., 2020).

Photographs of plant fossils were taken with a Nikon® Z7 digital camera with an Z 24-70mm f/4 S lens. The photographs of plant fossils and lithologies of the Xujiahe Formation were corrected only for contrast and sharpness using Adobe® Photoshop®. The line drawings of some plant fossils were produced using CorelDRAW® 2021. The selected specimens of plant fossils reported and figured here are housed in the Nanjing Institute of Geology and Palaeontology, Chinese Academy of Sciences, Nanjing, China with catalogue numbers: QLX2014103, QLX2014146, QLX2014159, QLX2014163, QLX2014170, QLX2014350, QLX2014399, QLX-2105-15U-542.

4 Results

4.1 Lithology

The Xujiahe Formation comprises seven lithological members (Members I-VII) in the studied section. Stratigraphic boundaries between each member and bed are distinct and they are easily recognized through lithological features (Figs. 2-A, B). The Xujiahe Formation is represented by a succession of dominant sandstone and mudstone beds, while, conglomerates, coal seams and thin layers of concretions were also deposited. Rock colors, sedimentary structures, coal accumulation and fossil preservation further reflect the Late Triassic depositional features.

(Fig. 2 is approximately here)

The members II, IV and VI of the Xujiahe Formation are dominated by thick sandstone beds, mostly medium to fine grained feldspathic-quartz and quartz sandstone, showing grayish to gray colors (Fig. 2-C). Carbonized plant branches are preserved in these sandstone beds (Fig. 2-D). A few coarse sandstone layers occur with quartz and/or chert gravels and with erosional surfaces (Fig. 3-A). Cross bedding is the most frequent and notable structure in the sandstone beds, usually associated with parallel bedding as well (Figs. 3-B, C). Climbing ripples are recorded in the members II and IV (Fig. 3-D). Wave-ripple marks and load-casts occur in the sandstone of the members II and VI (Figs. 3-E, F).

The members I, III, V and VII are dominated by gray to black mudstone and silty mudstone beds (Figs. 2-A, E, F). Variations in colors, between 'grey', 'dark grey' and 'black' are mainly dependent on the organic matter content, beds of these colors were mostly deposited in a coastal marsh (e.g., Member I) or peat swamp (e.g., Member VII), co-existing with coal seams. The horizontal and massive beddings of the mudstone beds are typically indicative for changing hydrodynamics and for supply of terrestrial clastics. Mudstones with preserved root-mucks and mud-cracks in Member I suggest that unconsolidated sediments were once exposed to relatively dry climate conditions (Figs. 3-G, 5-A). The *Skolithos*-type burrows of the Member III show a near-shore environment (Fig. 3-H). Some thin layers of siderite concretions are exposed in the mudstone beds of members I and V (Fig. 2-E), and two layers of calcic concretions are developed to the top of Member I.

(Fig. 3 is approximately here)

Conglomerate layers are exposed to the bottom of the sandstone beds, and some conglomerate lenses occur within sandstone beds (Figs. 2-G, 3-A). Quartzite and chert pebbles are common in conglomerate layers, indicating a long distance of transportation and/or flushing effects of high-energy flow. Fossil tree trunks are common observed in the conglomerate layers, as a result of flash flooding, debris flow events (Fig. 2-H).

Multiple thin coal seams occur in the mudstone members I, III, V and VII (Figs. 2-A, F), suggesting a reducing environment with abundant clastic sediments. The main industrial coal seams occur in Member VII (Fig. 2-F), and few coal seams of the Member V have also mining significance. Particular thin layers of siltstone and muddy siltstone occur as roof and floor shales.

4.2 Sedimentary facies and environment

The Xujiahe Formation of the Qilixia Section records a fluvial and lacustrine system (Fig. 4), while Member I records also a coastal marsh depositional system. These systems could be identified based on facies, subfacies and microfacies characters.

(Fig. 4 is approximately here)

The sandstone members record a well-developed meandering river system (e.g., members II and IV, Fig. 4). Associated riverbed microfacies is mainly represented by conglomerate and pebbly sandstone with clear erosional surfaces (e.g., the middle part of bed 04, Member II, Fig. 4). The typical retention sediments, including tree trunks and mud inclusions, are usually exposed as lenses to the bottom of erosional surfaces (Fig. 3-A). The marginal bank (point bar) microfacies is mainly represented by grayish, cross-bedded sandstone (e.g., the upper part of bed 04, Member II, Fig. 4). The levee microfacies is developed upward along the marginal banks, depositing fine-grained sandstone and siltstone. Flash floods destroyed levees and formed crevasse splay microfacies. Carbonized branches and mud interlayers are common in the sandstone beds of a crevasse splay (e.g., Fig. 2-D). The floodplain subfacies was generally developed to the top stage of a meandering river system or lateral it, consisting of siltstone and muddy siltstone. Horizontal beddings are common, and calcic concretions occur locally. The observed peat swamp was developed in a floodplain, with a limited preservation for channel lateral migration (e.g., bed 10, Member V, Fig. 4).

The fluvial delta plain facies expanded into a fluvial-lacustrine transition zone (e.g., Member V, Fig. 4). The distributary channel microfacies are mainly represented by fine-grained, well-sorted sandstone. Mud flames and tree trunks are common to the bottom of channel sandstone beds (e.g., bed 10, Member V, Fig. 4). The interdistributary bay microfacies are dominated by dark gray to black mudstone and carbonaceous mudstone, interlayered with thin-bedded siltstone. Plant fossils and siderite concretions are common in the interdistributary bay deposits (e.g., the lower part of bed 09, Member V, Fig. 4). Peat continuously accumulated in the swamps of a relatively stable delta plains, and which represents the important coal accumulating environments (e.g., the upper part of bed 09, Member V, Fig. 4).

The lacustrine system included of lakeshore and shallow lake subfacies (e.g., bed 16 and the lower part of bed 15, Member VII, Fig. 4). However, semi-deep and deep lake subfacies did not develop in the Qilixia Section locality. The lakeshore subfacies are dominated by gray-dark to black mudstone. Industrial coal seams were developed in the lakeshore swamp microfacies, containing fine-grained and thin bedded sandstone and siltstone beds (Fig. 2-F). The shallow lake subfacies are dominated by a thin-bedded gray mudstone, silty mudstone, and muddy siltstone. Some hydrophyte plant taxa (e.g., *Neocalamites*) and bivalves occur in the shallow lake deposits (Huang and Lu, 1992).

According to the occurrence of marine bivalve fossils in the western Sichuan Basin and to the occurrence of *Lingula* sp. in the eastern Sichuan Basin, the microfacies of Member I consists of lagoon, coastal marsh and estuarine sandbars (Gou, 1998; Wang et al., 2017; Fig. 4), as a result of the transgression and regression cycles during the latest Norian to the Rhaetian (Lu et al., 2015, 2019).

4.3 Floral community succession

The Xujiahe Flora has been reported throughout the Sichuan Basin, yielding well-preserved and highly diverse fossils, especially for the Qilixia Section and its surrounding areas (Ye et al., 1986; Wang et al., 2010; Fig. 5), counting 110 species of 59 genera of plant macrofossils (Ye et al., 1986;

Lu, 2019; Fig. 6, Table S1). Palynological studies of the Qilixia Section are extensive, reporting a high diversity of spores and pollen, counting 151 species of 64 genera (Li et al., 2016, 2020; Fig. 7).

(Figs. 5-8 are approximately here.)

Most of the plant fossils from Member I are too fragmentary to be investigated. According to palynological investigations, the dominant group of Member I are ferns (52.09~55.31%), followed by conifers (19.56~30.17%) and cycads/bennettites/ginkgophytes (8.94~14.97%) (Fig. 8). Some palynomorph environmental indicators (i.e., *Sulcusicystis* sp. and *Radicites* sp.) are also found in Member I (Lu et al., 2015; Li et al., 2016; Fig. 5-A), all indicating a coastal hydrophyte community (CHC) for Member I at this time (Fig. 6).

Plant macrofossils preserved in Member III suggest a community dominated by ferns, cycads, and horsetails (Fig. 6, Table S1). The palynological data also indicate the similar community composition, with dominant groups of ferns (51.06~64.33%) and cycads/bennettites/ginkgophytes (14.33~15.60%) (Fig. 8). The plant macrofossils and palynological data indicate a delta-plain wetland community (DWC) (Lu, 2019; Li et al., 2020). Compared with the CHC of Member I, the diversity of gymnosperms is higher in the DWC of Member III (Lu et al., 2019; Fig. 6).

Both macro- and micro-fossils are preserved in the lower beds of Member V (Figs. 5-C, D, E, F, and Fig. 8). However, the top of Member V yields only macrofossils and no palynomorphs (Fig. 8). The dominant groups include ferns (e.g., *Cladophlebis raciborskii*, *Todites* sp., Fig. 5-D, F), cycads (e.g., *Pterophyllum angustum*, Fig. 5-C), and ginkgophytes (e.g., *Ixostrobus* sp., Fig. 5-E). The proportion of fern spores is up to 71.78%, whereas the conifers is only 15.34% (sample QLX-10 of Bed 9, Member V; Fig. 8). Both the macro- and micro-fossils indicate a swamp wetland community (SWC) to have preserved in Member V (Lu, 2019; Li et al., 2020; Figs. 6 and 8).

Most fossil taxa of the Xujiahe Flora were found in Member VII, such as *Dictyophyllum nathorsti*, *Cladophlebis* sp., *Baiera elegans* and *Ginkgoites* sp. (Figs. 5-G, H, I, J). Both species and genera diversity of the plant macrofossils increase at first and then decrease (Fig. 6). The dominant groups changed from horsetails to ferns and cycads (Bed 15), and then to ginkgophytes and conifers (Bed 15 to 17) (Ye et al., 1986; Lu, 2019; Fig. 6). Meanwhile, the palynological data also show an upward decrease in ferns and an increase in gymnosperms (e.g., conifers, ginkgophytes) from Bed 15 to Bed 17 (Li et al., 2020; Fig. 8). This assemblage change reflects a transitional community succession (TCs), changing from lakeshore swamp to high lands that were preserved in Member VII (Figs. 6 and 8).

5 Discussion

5.1 Oscillations between fluvial and lacustrine depositional systems

Significant changes in term of palaeogeography, palaeoclimate and palaeoecology occurred in the Sichuan Basin throughout the Late Triassic. The Sichuan Basin occurred on the northern margin of the South China Block during the Late Triassic (Fig. 1-A). With the convergence of the South China Block, the North China Block, and the Indo-China Block (known as the Indosinian Movement), the Sichuan Basin was raised during the Middle- Late Triassic (Zhong et al., 1998). Due to the uplift of the Sichuan Basin, the westward retreat of the Tethys occurred and the Middle Triassic Leikoupo Formation was weathered during the Middle-Late Triassic in the Xuanhan area (Deng, 1996; Zhong et al., 1998; Wang et al., 2010). This large-scale regression was recorded by the sedimentary gap between the Middle Triassic Leikoupo Formation and the Upper Triassic Xujiahe Formation (Fig. 2-A).

Following the large-scale regression, a new transgressive episode started in the Carnian and influenced the Xuanhan area in the latest Norian (Lu et al., 2015). Thereafter, a coastal marsh began to take shape and the Xujiahe Formation deposited unconformably over the Leikoupo Formation remains (Fig. 2-A). Some thin layers of coal were accumulated, with the coincidental formation of calcic concretions and gypsum of Member I deposits, indicating a hot climate (Lu et al., 2015).

(Fig. 9 is approximately here)

With the continuous northward compression of the northern margin of the South China Block, the Qinling orogen to the north of the Sichuan Basin became raised and rivers originating from the Qinling orogen started to shape the topography of the Xuanhan area with sufficient terrigenous clastic sediments and water. The meandering rivers became the dominant sedimentary environment, as represented by the sequences of Member II. Repeated flood events, inferred from the regular occurrence of riverbed-point bar-natural levee associations, suggest regular heavy rain events in response to a megamonsoon development (Parrish and Peterson, 1988; Tian et al., 2016) (Fig. 9).

With the initial formation of the Sichuan Basin and the continuous deepening of the water at the study locality, the transition from channel to floodplain to lakeshore swamp was recorded in Member III (Figs. 4 and 9). However, the relatively stable environment didn't last long before the start of another episode of the Indosinian Movement (also known as the Anxian Movement, Wang, 1990). The tectonic activities not only promoted the continuous uplift of the Qinling Orogen, but also resulted in the uplift of the Longmenshan mountains, forming a prominent syntectonic conglomerate sequence near the source area (Wang, 2003; He, 2014; Liu et al., 2021). The fluvial dynamics of the surrounding orogens were therefore enhanced, providing sufficient terrigenous clastic sediments and water. The facies association of Member IV of the Qilixia Section recorded the Anxian Movement and its impact from a distance (Fig. 4).

With the tectonic activities tending to moderate, the environment became stable and the lake level became raised (Fig. 9). The wide deltaic flood-plain was formed in the middle Rhaetian (ca. 203~203.5 Ma, Fig. 9), with distributary channels and interdistributary bay deposits (Figs. 4 and 9). The coal accumulation was enhanced in a stable peat swamp of the interdistributary bay environment, and some thick, industry grade coal seams developed in the lower mudstone beds of Member V (e.g., upper part of Bed 9, Fig. 4).

Subsequently, the environment became disturbed again, as suggested by the mudstone breccia of the upper beds of Member V. The mudstone breccia composed of angular boulders suggest either an exceptional storm or even a tsunami event (Pole et al., 2018). Under this disturbed environment background, very few plant fossils could be preserved. Root clay and siderite concretions occurred in the upper beds of Member V, suggesting fluctuations of the lake level (Fig. 9). The disturbed environmental conditions extended throughout the upper Member V and the Member VI. The occurrence of both hummocky and swaley cross beddings in Member VI were proposed as strong evidence of more stormy conditions (Pole et al., 2018). The fine-grained and well-sorted quartz sandstone with wave-ripple marks of the Member VI may suggest a wave-dominated, near-shore environment.

Influenced by the lake transgression, a stable lakeshore and shallow lake environment developed prior to the Tr–J transition (Fig. 9). The depositional environment and facies evolution were mainly controlled by lake level changes. With the fall of lake level, a peat swamp environment occurred and the Xuanhan area became the coal depocenter, with industry grade, thick coal seams accumulated related to the stable environment conditions of Member VII (Fig. 2-F).

5.2 Palaeoclimate implications and ecological response

Species diversity, community composition and dominant taxa of the fossil assemblages can allow for inferences on palaeoclimate variations and palaeo-ecosystem stability (McElwain et al., 2007). Furthermore, syntheses of the sedimentary systems, community succession and major geological events contribute to better understanding of the ecological response of the Xujiahe Flora to the end-Triassic mass extinction and associated climatic and environmental change at that time (Fig. 9).

The observed water-level transgression across the wider depositional environment resulted in the formation of a transitional environment, which provided the initial habitats for the rise of the Xujiahe Flora in the latest Norian (ca. 207~207.2 Ma, Fig. 9). The thriving coastal hydrophyte community (CHC) of the Member I marked the origin of the Xujiahe Flora in the latest Norian in the

Xuanhan area. Both the community composition and the dominant taxa indicate hot and humid climatic conditions (Lu et al., 2019).

Subsequently, an environmentally disturbed floodplain developed during the uplift of the Qinling orogen across the Norian–Rhaetian transition (ca. 205~207 Ma, Fig. 9), terminating the favorable habitats for terrestrial plant ecosystems as described above. Locally, only the sphenopsid *Neocalamites* survived and became the dominant element, but *Podozamites* leaves, mainly transported and buried in the banks of lake or marshes, indicate a nearshore hydrophyte ecosystem as preserved in Member II (Huang and Lu, 1992). The occurrence of the fossil wood *Xenoxylon guangyuanensis* in the neighboring region of this basin was notable (Tian et al., 2016). Previously evidence suggests that the genus *Xenoxylon* was mainly distributed in the high latitude regions and reflecting cool and/or wet climate conditions, the southernmost occurrences of *Xenoxylon* in regions otherwise under warm or dry paleoclimates might indicate global colder/wetter climatic snaps (Philippe and Thévenard, 1996; Philippe et al., 2009). Therefore, the *X. guangyuanensis* would suggest a climatic cooling event linked to the development of the Late Triassic megamonsoon (Tian et al., 2016), influencing the evolution of gymnosperms.

Nearshore peat swamps developed as a result of lake level rise (Fig. 9). A community dominated by ferns, cycads and horsetails was thriving for a short period of time during the early Rhaetian (ca. 204.5 Ma, Fig. 9). The occurrence of ginkgophyte fossils (*Stachyopitys*) indicate that the climate was not as hot as during the latest Norian, and the delta plain wetlands community (DWC) of Member III represented the rise of the Xujiahe Flora in the early Rhaetian (Lu et al., 2019).

The second gap, induced by the Anxian Movement, influenced the floral communities again (Member VI, Fig. 9), coeval with the uplift of Longmenshan mountain-range towards the southwest, blocking the warm, moist water flow from the Tethys Ocean, deeply re-shaping local humidity patterns and the regional climate (Lu, 2019).

In the Middle Rhaetian (ca. 203~203.5 Ma, Beds 9 and 11 of Member V, Fig. 9), ferns and cycads were still dominant (Figs. 6 and 8). The ratio of fern spores was even as high as 71.78%, whereas the conifer pollen is only 15.34% (sample QLX-10 of Bed 9, Member V; Fig. 8). Both the macro- and micro- fossils indicate a swamp wetlands community (SWC) of the lower beds of Member V, growing under a warm and humid climate. Although the conifers and ginkgophytes showed higher diversity than the CHC of Member I and the DWC of Member III (Fig. 6), the abundance was still low and they were not the dominant groups.

Community destabilization marked the third gap of the floral succession at the study locality, suggesting a precursor interval of environmental stress in the late Rhaetian (ca. 202~203 Ma, Fig. 9). The mudstone breccia of Member V and the occurrence of both hummocky and swaley cross beddings in Member VI recorded the stormy conditions (Pole et al., 2018). The detrital charcoal fragments and inertinite recovered from the samples of the Xujiahe Formation also indicate a disturbed environment marked by intensive wildfire events (Pole et al., 2018; Lu, 2019). This ecosystem disturbance is also indicated by a series of discrete spikes in sulfide content and changes in planktonic community composition in the Panthalassic Ocean prior to the Tr–J boundary (Schoepfer et al., 2022).

Until the terminal Rhaetian, a stable nearshore environment became the refuge of the Xujiahe Flora in the Xuanhan area. Not only did the favorable habitats permitted the prosperity of the ferns, but also, it contributed to the diversification of conifers and ginkgophytes. Unlike the communities of the underlying members, the transitional community succession (TCs) of the Member VII showed an upward non-uniformity (Figs. 7, 8 and 9). Some hydrophyte taxa (e.g., *Neocalamites*) were preserved in the lowermost mudstone layers (TC-1), co-existing with some bivalve fossils (Ye et al., 1986; Huang and Lu, 1992). With the drop of the lake level, the shallow lake retreated and the lake shoreline changed, with the lakeshore subfacies becoming dominant. Within the lakeshore swamp microfacies, the wetland taxa became dominant in the Xuanhan area (TC-2). With the continuous drop of the lake level, the river dynamics became the main sedimentary feature and the flood plain expanded. Both the highland and the wetland taxa (i.e., conifers, ferns) were diverse and abundant in the middle mudstone layers of the Member VII (TC-2, 3). The bivalve fossils demonstrate the rise of lake level in the topmost bed of Member VII (Ye et al., 1986; Huang and Lu, 1992), with only a low-diversity floral community dominated by some upland xerophytic taxa (TC-4). The floral associations of the Member VII show an ecological collapse to the end of the Rhaetian (ca. 201.5~202 Ma, Fig. 9).

It is notable that the turnover from TC-2 to TC-3 and the ecological collapse is correlated with mercury enrichment prior to the Tr–J transition, as a CAMP global influence (Shen et al., 2022) (Fig. 9). Previous studies proposed that the Central Atlantic Magmatic Province (CAMP) volcanism have increased the frequency and scale of extreme climatic events (McElwain et al., 1999, 2007; Belcher et al., 2010), so that the enormous ecological pressure ultimately destroyed the terrestrial flora and generally their ecosystems (McElwain et al., 1999, 2007; Steinthorsdottir et al., 2012; Mander et al., 2013; Lindström et al., 2017; Capriolo et al., 2020; Yager et al., 2021). Recently, wildfire events across the Tr–J interval were identified at the Qilixia Section and throughout the whole basin (Pole et al., 2018; Lu, 2019; Song et al., 2020). Moreover, a multiproxy analysis (including organic carbon isotopes, mercury (Hg) concentrations and isotopes, chemical index of alteration (CIA), and clay minerals) of the Xujiahe Formation, across the Tr–J interval at Qilixia Section was undertaken (Shen et al., 2022). The increasing CIA in association with Hg peaks was interpreted as results of reflecting the volcanism-induced intensification of continental chemical weathering, which were linked with the CAMP event (Shen et al., 2022). Therefore, the ecological collapse in the end of the Rhaetian in the Xuanhan area was suggested to be largely induced by the CAMP emplacement and its associated climatic effects.

6 Conclusions

1) The Upper Triassic Xujiahe Formation yields the best record of the major changes of palaeogeography, palaeoclimate and palaeoecology occurring in the Late Triassic of the northeastern Sichuan Basin, South China. The oscillating fluvial-lacustrine depositional system during the late Triassic, and the sedimentary evolution of the basin were mainly controlled by the Indosinian Movement and by the regression-transgression cycle.
2) Within an overall warm and humid climate during the Late Triassic in the Xuanhan area, some climatic variations occurred, inferred from differences in floral communities of each member. The cooling and drying fluctuations influenced the diversification of gymnosperms.
3) Four communities and three obvious gaps document the rise and demise of Xujiahe Flora throughout the Late Triassic in the northeast Sichuan Basin. The floral community successions were closely related to sedimentary processes and to climatic variations. An ecosystem destabilization occurred in the Xuanhan area over one million years prior to the Tr–J interval, followed by an ecological collapse occurring at the Tr–J interval.
4) The Xujiahe Flora always recovered from the interruptions induced by tectonic movement, and it ultimately collapsed under the extreme climatic events and ecological pressure induced by the CAMP event.

Conflict of Interest

The authors declare that the research was conducted in the absence of any commercial or financial relationships that could be construed as a potential conflict of interest.

Author Contributions

YW, MEP and NL designed the study. NL, YX, LL, HC, XX, MR, MEP, WMK and YW carried out the field works. NL, YX and LL performed the lab works. NL, YX, LL and YW wrote the draft. All authors contributed to the interpretation and revision of the manuscript.

Funding

This study is financially supported by the National Natural Science Foundation of China (42202020, 41972120 and 42072009), and the Programs from State Key Lab of Palaeobiology and Stratigraphy (20191103, 213112).

Acknowledgments

We would like to thank Prof. Yue Li from Nanjing Institute of Geology and Palaeontology, Chinese Academy of Sciences for the suggestions regarding the manuscript. We appreciate Dr. Mingsong Li from Peking University and Senior Engineer Shuna Xi from the No. 137 Geological Survey of the Sichuan Coalfield Geology Bureau for their kind assistance during fieldtrips.

References

Atkinson, J.W., Wignall, P.B., Morton, J.D., Aze, T., and Hautmann, M. (2019). Body size changes in bivalves of the family Limidae in the aftermath of the end-Triassic mass extinction: the Brobdingnag effect. Palaeontology 62(4), 561-582. doi: 10.1111/pala.12415.

Barash, M.S. (2015). Abiotic causes of the great mass extinction of marine biota at the Triassic-Jurassic boundary. Oceanology 55(3), 374-382. doi: 10.1134/s0001437015030017.

Barbacka, M., Pacyna, G., Kocsis, Á.T., Jarzynka, A., Ziaja, J., and Bodor, E. (2017). Changes in terrestrial floras at the Triassic-Jurassic Boundary in Europe. Palaeogeography, Palaeoclimatology, Palaeoecology 480, 80-93. doi: 10.1016/j.palaeo.2017.05.024.

Belcher, C.M., Mander, L., Rein, G., Jervis, F.X., Haworth, M., Hesselbo, S.P., et al. (2010). Increased fire activity at the Triassic/Jurassic boundary in Greenland due to climate-driven floral change. Nature Geoscience 3(6), 426-429. doi: 10.1038/ngeo871.

Benton, M.J. (1986). More than one event in the late Triassic mass extinction. Nature 321(6073), 857-861. doi: 10.1038/321857a0.

Benton, M.J. (1995). Diversification and extinction in the history of life. Science 268(5207), 52-58. doi: 10.1126/science.7701342.

Capriolo, M., Marzoli, A., Aradi, L.E., Callegaro, S., Dal Corso, J., Newton, R.J., et al. (2020). Deep CO_2 in the end-Triassic Central Atlantic Magmatic Province. Nature communications 11(1), 1670. doi: 10.1038/s41467-020-15325-6.

Cascales-Miňana, B., and Cleal, C.J. (2012). Plant fossil record and survival analyses. Lethaia 45(1), 71-82. doi: 10.1111/j.1502-3931.2011.00262.x.

Cleveland, D.M., Nordt, L.C., Dworkin, S.I., and Atchley, S.C. (2008). Pedogenic carbonate isotopes as evidence for extreme climatic events preceding the Triassic-Jurassic boundary: Implications for the biotic crisis? Geological Society of America Bulletin 120(11-12), 1408-1415. doi: 10.1130/b26332.1.

Deng, K. (1996). “Formation and development of Sichuan Basin," in Sichuan Basin Formation and Development, ed. Z. Guo. (Beijing: Geilogical Publishing House), 113-138.

Fowell, S.J., and Olsen, P.E. (1993). Time calibration of Triassic/Jurassic microfloral turnover, eastern North America. Tectonophysics 222(3-4), 361-369. doi: 10.1016/0040-1951(93)90359-r.

Götz, A.E., Ruckwied, K., Pálfy, J., and Haas, J. (2009). Palynological evidence of synchronous changes within the terrestrial and marine realm at the Triassic/Jurassic boundary (Csővár section, Hungary). Review of Palaeobotany and Palynology 156(3-4), 401-409. doi: 10.1016/j.revpalbo.2009.04.002.

Gou, Z. (1998). The Bivalve Faunas from the Upper Triassic Xujiahe Formation in the Sichuan Basin. Sedimentary Facies and Palaeogeography 18(2), 20-29.

Hallam, A. (2002). How catastrophic was the end-Triassic mass extinction? Lethaia 35(2), 147-157. doi: 10.1080/002411602320184006.

He, L. (2014). Permian to Late Triassic evolution of the Longmen Shan Foreland Basin (Western Sichuan): Model results from both the lithospheric extension and flexure. Journal of Asian Earth Sciences 93, 49-59. doi: 10.1016/j.jseaes.2014.07.007.

He, T., Dal Corso, J., Newton, R.J., Wignall, P.B., Mills, B.J.W., Todaro, S., et al. (2020). An enormous sulfur isotope excursion indicates marine anoxia during the end-Triassic mass extinction. Science Advances 6(37), eabb6704. doi: 10.1126/sciadv.abb6704.

Hesselbo, S.P., McRoberts, C.A., and Pálfy, J. (2007). Triassic–Jurassic boundary events: Problems, progress, possibilities. Palaeogeography, Palaeoclimatology, Palaeoecology 244(1), 1-10. doi: 10.1016/j.palaeo.2006.06.020.

Hesselbo, S.P., Robinson, S.A., Surlyk, F., and Piasecki, S. (2002). Terrestrial and marine extinction at the Triassic-Jurassic boundary synchronized with major carbon-cycle perturbation: A link to initiation of massive volcanism? Geology 30(3), 251-254. doi: 10.1130/0091-7613(2002)030<0251:Tameat>2.0.Co;2.

Huang, Q. (1995). Palaeoclimate and coal-forming characteristics of the Late Triassic Xujiahe Stage in northern Sichuan. Geological Review 41(1), 92-99.

Huang, Q., and Lu, S. (1992). The Primary Studies on the Palaeoecology of the Late Triassic Xujiahe Flora in Eastern Sichuan. Earth Science-Journal of China University of Geosciences 17(3), 329-335.

Korte, C., Ruhl, M., Ullmann, C.V., and Hesselbo, S.P. (2019). "Chemostratigraphy Across the Triassic–Jurassic Boundary," in Chemostratigraphy Across Major Chronological Boundaries, eds. A.N. Sial, C. Gaucher, M. Ramkumar & V.P. Ferreira. (US: American Geophysical Union), 185-210.

Kürschner, W.M., Bonis, N.R., and Krystyn, L. (2007). Carbon-isotope stratigraphy and palynostratigraphy of the Triassic–Jurassic transition in the Tiefengraben section — Northern Calcareous Alps (Austria). Palaeogeography, Palaeoclimatology, Palaeoecology 244(1), 257-280. doi: 10.1016/j.palaeo.2006.06.031.

Kustatscher, E., Ash, S.R., Karasev, E., Pott, C., Vajda, V., Yu, J., et al. (2018). "Flora of the Late Triassic," in The Late Triassic World, ed. H. Tanner Lawrence. Springer), 545-622.

Li, J., Huang, C., Wen, X., and Zhang, M. (2021). Mesozoic paleoclimate reconstruction in Sichuan Basin, China: Evidence from deep-time paleosols. Acta Sedimentologica Sinica 39(5), 1157-1170. doi: 10.14027/j.issn.1000-0550.2020.058.

Li, L., Wang, Y., Kürschner, W.M., Ruhl, M., and Vajda, V. (2020). Palaeovegetation and palaeoclimate changes across the Triassic–Jurassic transition in the Sichuan Basin, China. Palaeogeography, Palaeoclimatology, Palaeoecology 556, 109891. doi: 10.1016/j.palaeo.2020.109891.

Li, L., Wang, Y., Liu, Z., Zhou, N., and Wang, Y. (2016). Late Triassic palaeoclimate and palaeoecosystem variations inferred by palynological record in the northeastern Sichuan Basin, China. PalZ 90(2), 327-348. doi: 10.1007/s12542-016-0309-5.

Li, L., Wang, Y., Vajda, V., and Liu, Z. (2018). Late Triassic ecosystem variations inferred by palynological records from Hechuan, southern Sichuan Basin, China. Geological Magazine 155(8), 1793-1810. doi: 10.1017/s0016756817000735.

Li, M., Zhang, Y., Huang, C., Ogg, J., Hinnov, L., Wang, Y., et al. (2017). Astronomical tuning and magnetostratigraphy of the Upper Triassic Xujiahe Formation of South China and Newark

Supergroup of North America: Implications for the Late Triassic time scale. Earth and Planetary Science Letters 475, 207-223. doi: 10.1016/j.epsl.2017.07.015.

Lindström S., van de Schootbrugge B., Hansen K.H., Pedersen, G.K., Alsen, P., Thibault, N., Dybkjær, K., Bjerrum, C.J., Nielsen, L.H. (2017). A new correlation of Triassic–Jurassic boundary successions in NW Europe, Nevada and Peru, and the Central Atlantic Magmatic Province: A time-line for the end-Triassic mass extinction. Palaeogeography, Palaeoclimatology, Palaeoecology. 478: 80-102. doi.org/10.1016/j.palaeo.2016.12.025.

Liu, S., Yang, Y., Deng, B., Zhong, Y., Wen, L., Sun, W., et al. (2021). Tectonic evolution of the Sichuan Basin, Southwest China. Earth-Science Reviews 213. doi: 10.1016/j.earscirev.2020.103470.

Liu, Z., Li, L., and Wang, Y. (2015). Late Triassic spore-pollen assemblage from Xuanhan of Sichuan, China. Acta Micropalaeontologica Sinica 32(1), 43-62. doi: 10.16087/j.cnki.1000-0674.20150407.006.

Lee, P.-C. (1964). Fossil plants from the Hsuchiaho Series od Kwangyüan, northern Szechuan. Memoirs of Institute of Geology and Palaeontology, Academia Sinica (3), 101-178.

Lu, N. (2019). Changes in sedimentary environment and terrestrial paleoecology across the Triassic-Jurassic transition in eastern Sichuan Basin. doctoral thesis, University of Science and Technology of China.

Lu, N., Li, Y., Wang, Y., Xu, Y., and Zhou, N. (2021). Fossil dipterid fern *Thaumatopteris* in China: new insights of systematics, diversity and tempo-spatial distribution patterns. Historical Biology 33(10), 2316-2329. doi: 10.1080/08912963.2020.1791106.

Lu, N., Wang, Y., Popa, M.E., Xie, X., Li, L., Xi, S., et al. (2019). Sedimentological and paleoecological aspects of the Norian–Rhaetian transition (Late Triassic) in the Xuanhan area of the Sichuan Basin, Southwest China. Palaeoworld 28(3), 334-345. doi: 10.1016/j.palwor.2019.04.006.

Lu, N., Xie, X., Wang, Y., and Li, L. (2015). The Analysis of Sedimentary Environmental Evolution of the T3x/T2l Boundary Transition in Qilixia of Xuanhan, Sichuan. Acta Sedimentologica Sinica 33(6), 1149-1158.

Lucas, S.G., and Tanner, L.H. (2015). End-Triassic nonmarine biotic events. Journal of Palaeogeography 4(4), 331-348. doi: 10.1016/j.jop.2015.08.010.

Lucas, S.G., and Tanner, L.H. (2018). "The Missing Mass Extinction at the Triassic-Jurassic Boundary," in The Late Triassic World, ed. H. Tanner Lawrence. Springer), 721-785.

Mander, L., Kürschner, W.M., and McElwain, J.C. (2013). Palynostratigraphy and vegetation history of the Triassic–Jurassic transition in East Greenland. Journal of the Geological Society 170(1), 37-46. doi: 10.1144/jgs2012-018.

Marzoli, A., Bertrand, H., Knight, K.B., Cirilli, S., Buratti, N., Vérati, C., et al. (2004). Synchrony of the Central Atlantic magmatic province and the Triassic-Jurassic boundary climatic and biotic crisis. Geology 32(11). doi: 10.1130/g20652.1.

McElwain, J.C., Beerling, D.J., and Woodward, F.I. (1999). Fossil plants and global warming at the Triassic-Jurassic boundary. Science 285(5432), 1386-1390. doi: 10.1126/science.285.5432.1386.

McElwain, J.C., Popa, M.E., Hesselbo, S.P., Haworth, M., and Surlyk, F. (2007). Macroecological responses of terrestrial vegetation to climatic and atmospheric change across the Triassic/Jurassic boundary in East Greenland. Paleobiology 33(4), 547-573. doi: 10.1666/06026.1.

McElwain, J.C., and Punyasena, S.W. (2007). Mass extinction events and the plant fossil record. Trends in Ecology and Evolution 22(10), 548-557. doi: 10.1016/j.tree.2007.09.003.

Mihca, R., Bonis N.R., Reichart, G.-J., Damsté J.S.S., and Kürschner W.M., (2011). Atmospheric Carbon Injection Linked to End-Triassic Mass Extinction. Science 333(6041), 430-434.

Ruhl, M., Hesselbo, S.P., Al-Suwaidi, A., Jenkyns, H.C., Damborenea, S.E., Manceñido, M.O., Storm, M., Mather, T.A., and Riccardi, A.C. (2020). On the onset of Central Atlantic Magmatic Province (CAMP) volcanism and environmental and carbon-cycle change at the Triassic–Jurassic transition (Neuquén Basin, Argentina). Earth-Science Reviews 208, 103229. doi.org/10.1016/j.earscirev.2020.103229.

Michalík, J., Lintnerová, O., Gaździcki, A., and Soták, J. (2007). Record of environmental changes in the Triassic–Jurassic boundary interval in the Zliechov Basin, Western Carpathians. Palaeogeography, Palaeoclimatology, Palaeoecology 244(1), 71-88. doi: 10.1016/j.palaeo.2006.06.024.

Olsen, P.E., Kent, D.V., Sues, H.D., Koeberl, C., Huber, H., Montanari, A., et al. (2002). Ascent of dinosaurs linked to an iridium anomaly at the Triassic-Jurassic boundary. Science 296(5571), 1305-1307. doi: 10.1126/science.1065522.

Parrish, J.T., and Peterson, F. (1988). Wind directions predicted from global circulation models and wind directions determined from eolian sandstones of the western United States-a comparison. Sedimentary Geology 56(1-4), 261–282.

Percival, L.M.E., Ruhl, M., Hesselbo, S.P., Jenkyns, H.C., Mather, T.A., and Whiteside, J.H. (2017). Mercury evidence for pulsed volcanism during the end-Triassic mass extinction. Proceedings of the National Academy of Sciences 114(30), 7929. doi: 10.1073/pnas.1705378114.

Philippe, M., Thévenard, F. (1996). Repartition and palaeoecology of the Mesozoic wood genus Xenoxylon: palaeoclimatological implications for the Jurassic of Western Europe. Review of Palaeobotany and Palynology 91(1-4), 353–370. doi: 10.1016/0034-6667(95)00067-4

Philippe, M., Jiang, H.E., Kim, K., Oh, C., Gromyko, D., Harland, M., Paik, I.S., Thévenard, F. (2009). Structure and diversity of the Mesozoic wood genus Xenoxylon in Far East Asia: implications for terrestrial palaeoclimates. Lethaia 42(4), 393–406. Doi: 10.1111/j.1502-3931.2009.00160.x.

Pole, M., Wang, Y., Dong, C., Xie, X., Tian, N., Li, L., et al. (2018). Fires and storms—a Triassic–Jurassic transition section in the Sichuan Basin, China. Palaeobiodiversity and Palaeoenvironments 98(1), 29-47. doi: 10.1007/s12549-017-0315-y.

Raup, D.M., and Sepkoski, J.J. (1982). Mass extinctions in the marine fossil record. Science 215(4539), 1501-1503. doi: 10.1126/science.215.4539.1501.

Schoepfer, S.D., Shen, J., Sano, H., and Algeo, T.J. (2022). Onset of environmental disturbances in the Panthalassic Ocean over one million years prior to the Triassic-Jurassic boundary mass extinction. Earth-Science Reviews 224, 103870.

Sepkoski, J.J. (1981). A factor analytic description of the Phanerozoic marine fossil record. Paleobiology 7(1), 36-53.

Shen, J., Yin, R., Zhang, S., Algeo, T.J., Bottjer, D.J., Yu, J., Xu, G., Penman, D., Wang, Y., Li, L., Shi, X., Planavsky, N.J., Feng, Q., and Xie, S. (2022). Intensified continental chemical weathering and carbon-cycle perturbations linked to volcanism during the Triassic–Jurassic transition. Nature Communications 13, 299. doi: 10.1038/s41467-022-27965-x.

Song, Y., Algeo, T.J., Wu, W., Luo, G., Li, L., Wang, Y., et al. (2020). Distribution of pyrolytic PAHs across the Triassic-Jurassic boundary in the Sichuan Basin, southwestern China:

Evidence of wildfire outside the Central Atlantic Magmatic Province. Earth-Science Reviews 201, 102970. doi: 10.1016/j.earscirev.2019.102970.

Stanley, G.D., Jr., Shepherd, H.M.E., and Robinson, A.J. (2018). Paleoecological Response of Corals to the End-Triassic Mass Extinction: An Integrational Analysis. Journal of Earth Science 29(4), 879-885. doi: 10.1007/s12583-018-0793-5.

Steinthorsdottir, M., Woodward, F.I., Surlyk, F., and McElwain, J.C. (2012). Deep-time evidence of a link between elevated CO_2 concentrations and perturbations in the hydrological cycle via drop in plant transpiration. Geology 40(9), 815-818. doi: 10.1130/g33334.1.

Sun, G., Meng, F., Qian, L., and Ouyang, S. (1995). "Triassic floras," in Fossil floras of China through the geological ages, ed. X. Li. (Guangzhou, China: Guangdong Science and Technology Press), 305-342.

Tian, N., Wang, Y., Philippe, M., Li, L., Xie, X., and Jiang, Z. (2016). New record of fossil wood *Xenoxylon* from the Late Triassic in the Sichuan Basin, southern China and its paleoclimatic implications. Palaeogeography, Palaeoclimatology, Palaeoecology 464, 65-75. doi: 10.1016/j.palaeo.2016.02.006.

Tomašových, A., and Siblík, M. (2007). Evaluating compositional turnover of brachiopod communities during the end-Triassic mass extinction (Northern Calcareous Alps): Removal of dominant groups, recovery and community reassembly. Palaeogeography, Palaeoclimatology, Palaeoecology 244(1), 170-200. doi: 10.1016/j.palaeo.2006.06.028.

Van de Schootbrugge, B., Quan, T.M., Lindström, S., Püttmann, W., Heunisch, C., Pross, J., et al. (2009). Floral changes across the Triassic/Jurassic boundary linked to flood basalt volcanism. Nature Geoscience 2(8), 589-594. doi: 10.1038/ngeo577.

Wang, C., Zheng, R., Li, S., Li, S., Li, G., et al. (2017). Stratigraphic Subdivision and Correlation of the Upper Triassic Xujiahe Formation, Eastern Sichuan Basin: A Case Study of the Woxinshuang Area. Journal of Stratigraphy 41(1), 94-102.

Wang, J. (1990). Anxian tectonic movement. Oil & Gas Geology 11(3), 223-234.

Wang, J. (2003). Recognition on the main episode of Indo-China Movement in the Longmen Moutains. Acta Geologica Sichuan 23(2), 65-69.

Wang, Y., Fu, B., Xie, X., Huang, Q., Li, K., Li, G., et al. (2010). The Terrestrial Triassic and Jurassic Systems in the Sichuan Basin, China. Hefei, China: University of Sicence and Technology of China Press.

Wang, Y., Li, L.Q., Guignard, G., Dilcher, D.L., Xie, X., Tian, N., et al. (2015). Fertile structures with in situ spores of a dipterid fern from the Triassic in southern China. Journal of Plant Research 128(3), 445-457. doi: 10.1007/s10265-015-0708-9.

Whiteside, J.H., Olsen, P.E., Eglinton, T., Brookfield, M.E., and Sambrotto, R.N. (2010). Compound-specific carbon isotopes from Earth's largest flood basalt eruptions directly linked to the end-Triassic mass extinction. Proc Natl Acad Sci U S A 107(15), 6721-6725. doi: 10.1073/pnas.1001706107.

Williford, K.H., Foriel, J., Ward, P.D., and Steig, E.J. (2009). Major perturbation in sulfur cycling at the Triassic-Jurassic boundary. Geology 37(9), 835-838. doi: 10.1130/g30054a.1.

Wotzlaw, J.F., Guex, J., Bartolini, A., Gallet, Y., Krystyn, L., McRoberts, C.A., et al. (2014). Towards accurate numerical calibration of the Late Triassic: High-precision U-Pb geochronology constraints on the duration of the Rhaetian. Geology 42(7), 571-574. doi: 10.1130/g35612.1.

Wu, S. (1983). “On the Late Triassic and Early-Middle Jurassic Floras and Their Distributions in China," in Palaeobiogeographic Provinces of China, ed. E.C.o.F.T.o.P.B. Series. (Beijing: Science Press), 121-130.

Wu, S. (1999). Upper Triassic plants from Sichuan. Bulletin of Nanjing Institute of Geology and Palaeontology, Academia Sinica (14), 1-69.

Xu, Y., Popa, M.E., Zhang, T., Lu, N., Zeng, J., Zhang, X., et al. (2021). Re-appraisal of *Anthrophyopsis* (Gymnospermae): New material from China and global fossil records. Review of Palaeobotany and Palynology 292. doi: 10.1016/j.revpalbo.2021.104475.

Yager, J.A., West, A.J., Thibodeau, A.M., Corsetti, F.A., Rigo, M., Berelson, W.M., Bottjer, D.J., Greene, S.E., Ibarra, Y., Jadoul, F., Ritterbush, K.A., Rollins, N., Rosas, S., Di Stefano, P., Sulca, D., Todaro, S., Wynn, P., Zimmermann, L., Bergquist, B.A. (2021). Mercury contents and isotope ratios from diverse depositional environments across the Triassic–Jurassic Boundary: Towards a more robust mercury proxy for large igneous province magmatism. Earth-Science Reviews 223, 103775. doi.org/10.1016/j.earscirev.2021.103775.

Ye, M., Liu, X., Huang, G., Chen, L., Peng, S., et al. (1986). Late Triassic and Early-Middle Jurassic Fossil Plants from Northeastern Sichuan. Hefei: Anhui Science and Technology Publishing House.

Zhong, D. (1998). Paleotethysides of the western Guizhou-Sichuan region. Beijing: Science Press

Zhu, M., Chen, H., Zhou, J., and Yang, S. (2017). Provenance change from the Middle to Late Triassic of the southwestern Sichuan basin, Southwest China: Constraints from the sedimentary record and its tectonic significance. Tectonophysics 700-701, 92-107. doi: 10.1016/j.tecto.2017.02.006.

Figure Captions

Fig. 1 Maps showing the location of the Qilixia Section, NE Sichuan Basin, China.

A. The palaeogeographic location of Sichuan Basin during the Rhaetian (Base map after Metcalfe, 2011); **B**. The location of the Qilixia Section, NE Sichuan Basin; **C**. Simplified geological map of the Qilixia Section and surrounding region (after Sichuan Bureau of Geology, 1980).

Fig. 2 Stratigraphic boundaries and lithologies of the Xujiahe Formation at the Qilixia Section.

A. The lithological boundary between the Upper Triassic Xujiahe Formation and the Middle Triassic Leikoupo Formation; **B**. The lithological boundary between the Lower Jurassic Zhenzhuchong Formation and the Upper Triassic Xujiahe Formation; **C**. The massive sandstone bed of Member II; **D**. The sandstone bed with carbonized branches of Member IV; **E**. The mudstone bed with siderite concretions of Member I; **F**. The fossils bearing layers and coal seam of Member VII; **G**. The conglomerate layer of Member II; **H**. The conglomerate layer with tree trunks of Member II.

Fig. 3 Sedimentary structures of the Xujiahe Formation at the Qilixia Section.

A. The sandstone bed with conglomerate lens and erosion surface of Member II; **B**. The parallel beddings of Member IV; **C**. The cross beddings of Member VI; **D**. The climbing ripples of Member IV; **E**. The wave-ripple marks of Member VI; **F**. The load casts of Member II; **G**. The mud cracks of Member I; **H**. The *Skolithos* burrows of Member III (after Pole et al., 2018).

Fig. 4 Detailed log showing the lithology, sedimentary structures, fossil preservation and sedimentary sequences of the Xujiahe Formation at the Qilixia Section.

Fig. 5 Representatives of the Xujiahe Flora collected from the Qilixia Section.

A. *Radicites* sp., Member I, QLX2014103; **B**. *Neocalamites* sp., Member II; **C**. *Pterophyllum angustum* (Braun) Gothan, Member V, QLX2014163; **D**. *Cladophlebis raciborskii* Zeiller, Member V, QLX2014146; **E**. 01, *Ixostrobus* sp.; 02, *Podozamites* sp., Member V, QLX2014159; **F**. *Cladophlebis* sp., Member V, QLX2014170; **G**. *Baiera elegans* Oishi, QLX2014350; **H.** *Ginkgoites sibiricus* (Heer) Seward, Member VII, QLX-2105-15U-542; **I.** *Cladophlebis* sp., Member VII, QLX2014399; **J.** *Dictyophyllum nathorsti* Zeiller, Member VII, QLX-2105-15U-680a. (A, C-J, scale bar = 10 mm; B, scale bar = 50 mm; The plant fossils are showing in the stratigraphic order).

Fig. 6 Stratigraphic occurrences of the plant macrofossils and division of the floral communities of the Late Triassic Xujiahe Flora.

*The division of the floral communities are based on the plant macrofossils and palynological data.

Fig. 7 Representative spore and pollen taxa recovered from the Xujiahe Formation at the Qilixia section.

A. *Sphagnumsporites clavus* (Balme, 1957) Huang, 2000, Member I, QLX-1-1; **B**. *Sphagnumsporites perforates* (Leschik) Liu, 1986, Member I, QLX-1-4; **C**. *Cibotiumspora robusta* Lu et Wang, 1983, Member I, QLX-1-1; **D**. *Dictyophyllidites harrisii* Couper, 1958, Member I, QLX-1-1; **E**. *Toroisporis minoris* (Nakoman) Sun et He, 1980, Member I, QLX-1-3; **F,** *Toroisporis minoris* (Nakoman) Sun et He, 1980, Member III, QLX-7-7; **G.** *Concavisporites toralis* (Leschik, 1955) Nilsson, 1958, Member I, QLX-1-3; **H.** *Cyathidites minor* Couper, 1953, Member I, QLX-1-4; **I.** *Osmundacidites granulata* (Mal.) Zhou, 1981, Member I, QLX-2-1; **J.** *Cyclogranisporites arenosus* Madler, 1964, Member III, QLX-8-2; **K.** *Angiopteridaspora denticulata* Chang, 1965, Member I, QLX-1-1; **L.** *Granulatisporites triconvexus* Staplin, 1960, Member I, QLX-1-4; **M.** *Osmundacidites wellmanii* Couper, 1953, Member III, QLX-9-2; **N.** *Planisporites dilucidus* Megregor, 1960, Member V, QLX-12-2; **O.** *Araucariacites australis* Cookson, 1947, Member I, QLX-1-3; **P.** *Alisporites parvus* De Jersey, 1962, Member VII, XHQL-89-5; **Q.** *Alisporites parvus* De Jersey, 1962, Member

VII, XHQL-91-1; **R.** *Vitreisporites pallidus* (Reissinger) Nilsson, 1958, Member II, XHQL-40-2; **S.** *Pinuspollenites divulgatus* (Bolkh.) Qu, 1980, Member VII, XHQL-91-1; **T.** *Pinuspollenites alatipollenites* (Rouse) Liu, 1982, Member VII, XHQL-91-1; **U.** *Piceites enodis* Bolkhovitina, 1956, Member II, QLX-2-1; **V.** *Quadraeculina anellaeformis* Maljavkina, 1949, Member VII, XHQL-89-1; **W.** *Podocarpidites unicus* (Bolkh.) Pocock, 1970, Member II, XHQL-40-1; **X.** *Cycadopites parvus* (Bolkh.) Pocock, 1970, Member I, QLX-1-1; **Y.** *Cycadopites follicularis* Wilson et Webster, 1946, Member II, XHQL-40-2; **Z.** *Cycadopites reticulata* (Nilsson) Arjang, 1975, Member VII, XHQL-91-1; **AA.** *Monosulcites granulatus* Couper 1960, Member VII, XHQL-91-1; **AB.** *Monosulcites minimus* Cookson, 1947, Member I, QLX-1-4; **AC.** *Monosulcites enormis* Jain, 1968, Member VII, XHQL-89-3. (scale bar = 20 μm)

Fig. 8 Stratigraphic occurrences and abundance diagram of major spore-pollen groups recovered from the Xujiahe Formation at the Qilixia section.

Fig. 9 Environmental oscillations and the ecological responses of the Xujiahe Formation at the Qilixia Section.

1). The 405-kyr eccentricity cycle and ages are from Li et al., 2017. **2)**. The initial- and main- carbon isotope excursions and mercury (Hg) isotope enrichment are from Shen et al., 2022.

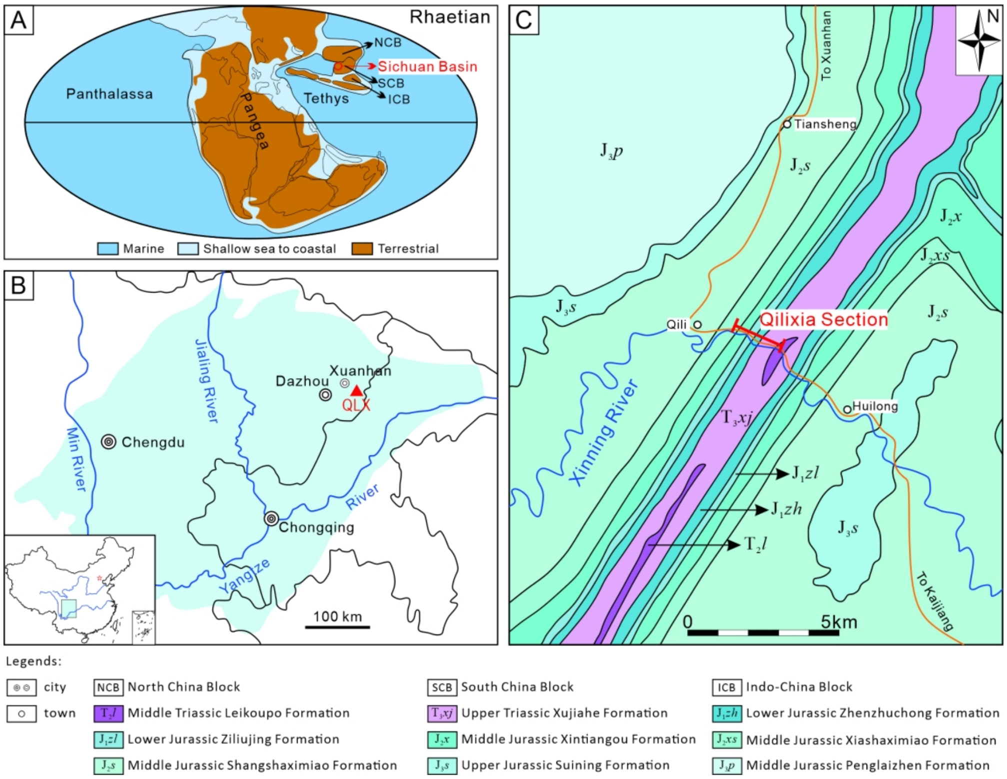

172x132mm (300 x 300 DPI)

180x226mm (300 x 300 DPI)

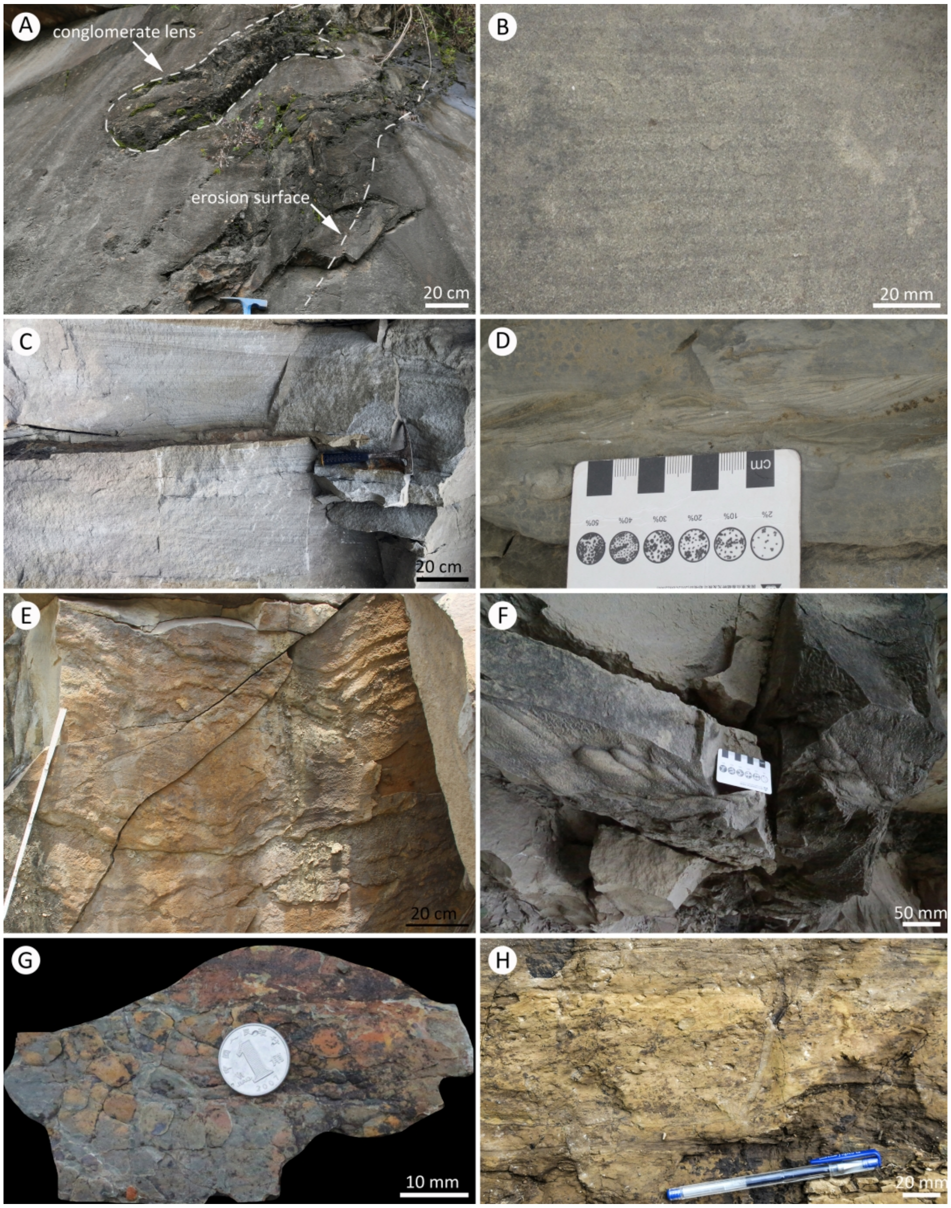

209x266mm (300 x 300 DPI)

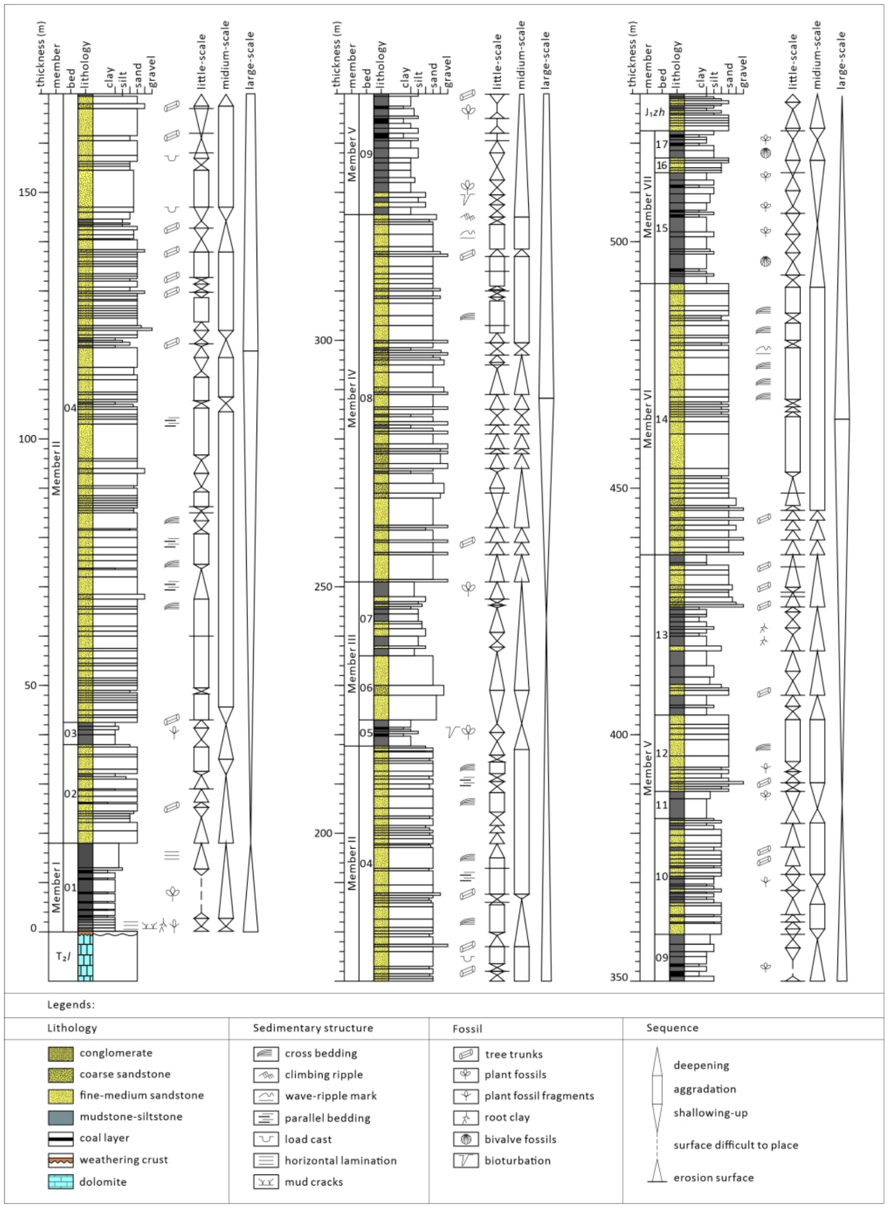

178x243mm (300 x 300 DPI)

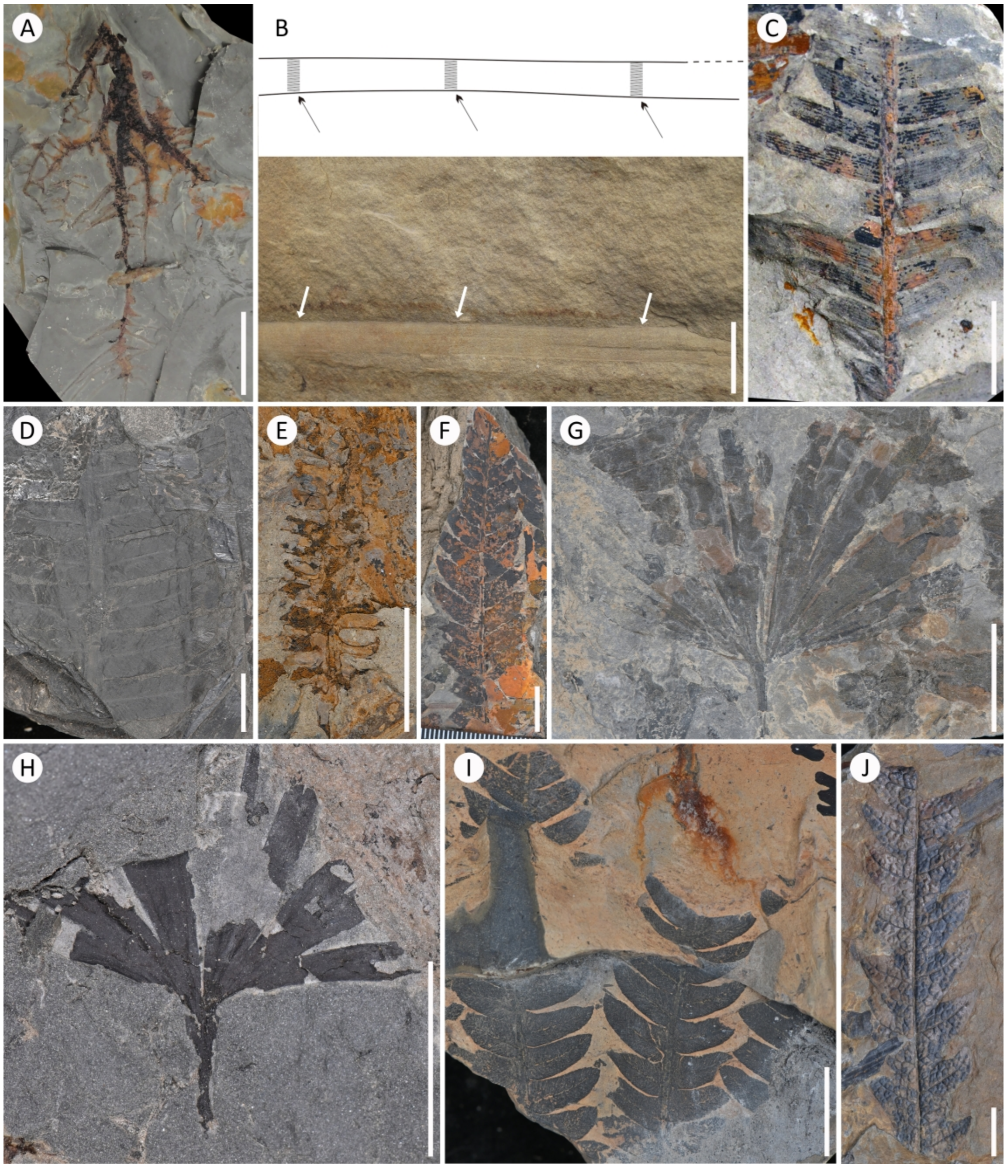

1750x2029mm (72 x 72 DPI)

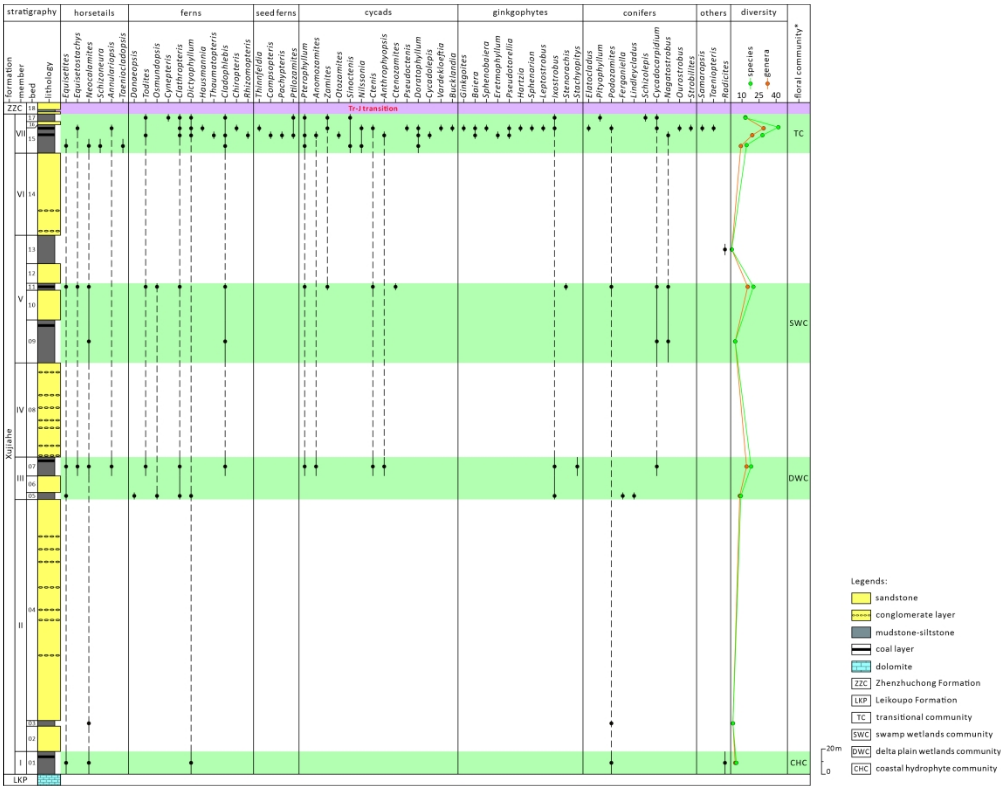

263x206mm (300 x 300 DPI)

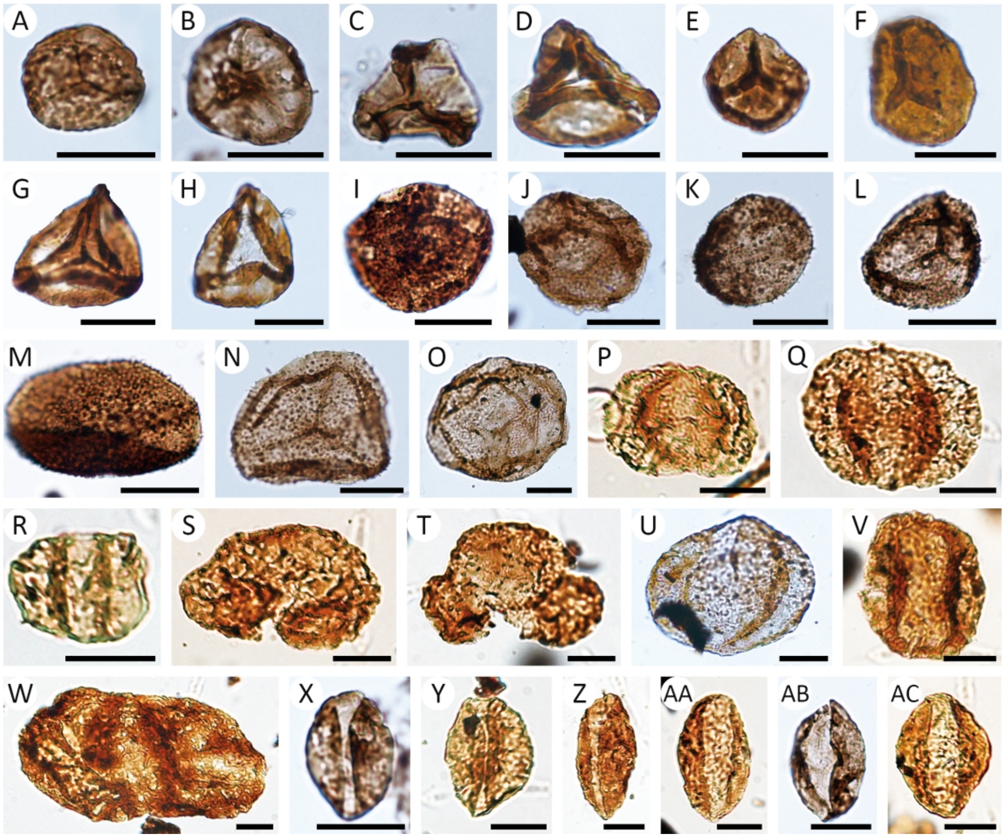

784x652mm (72 x 72 DPI)

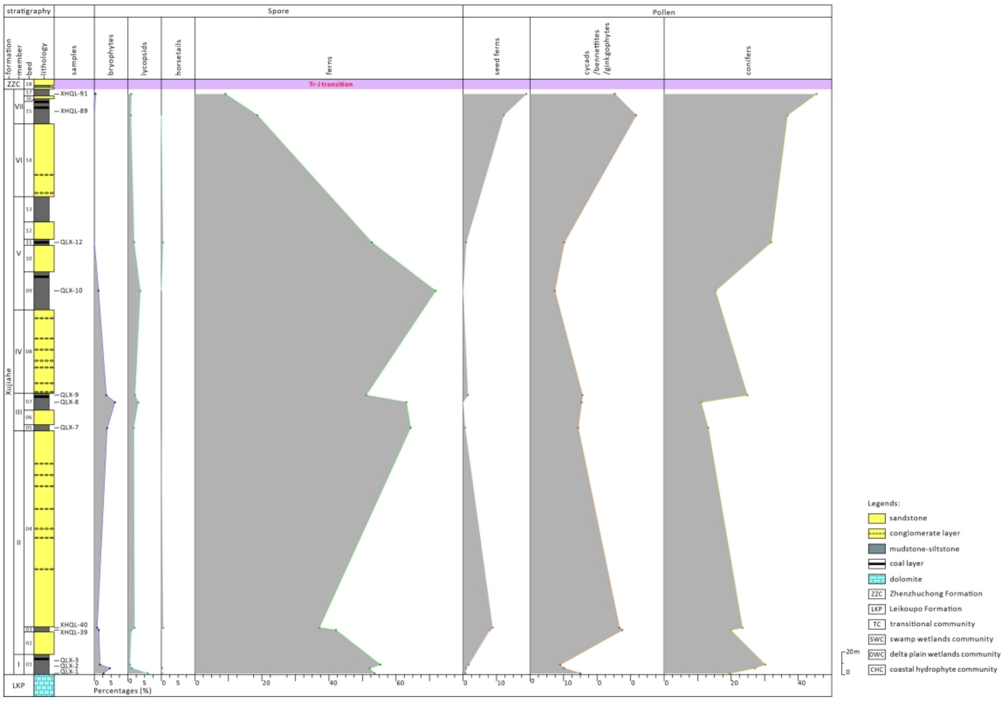

297x206mm (300 x 300 DPI)

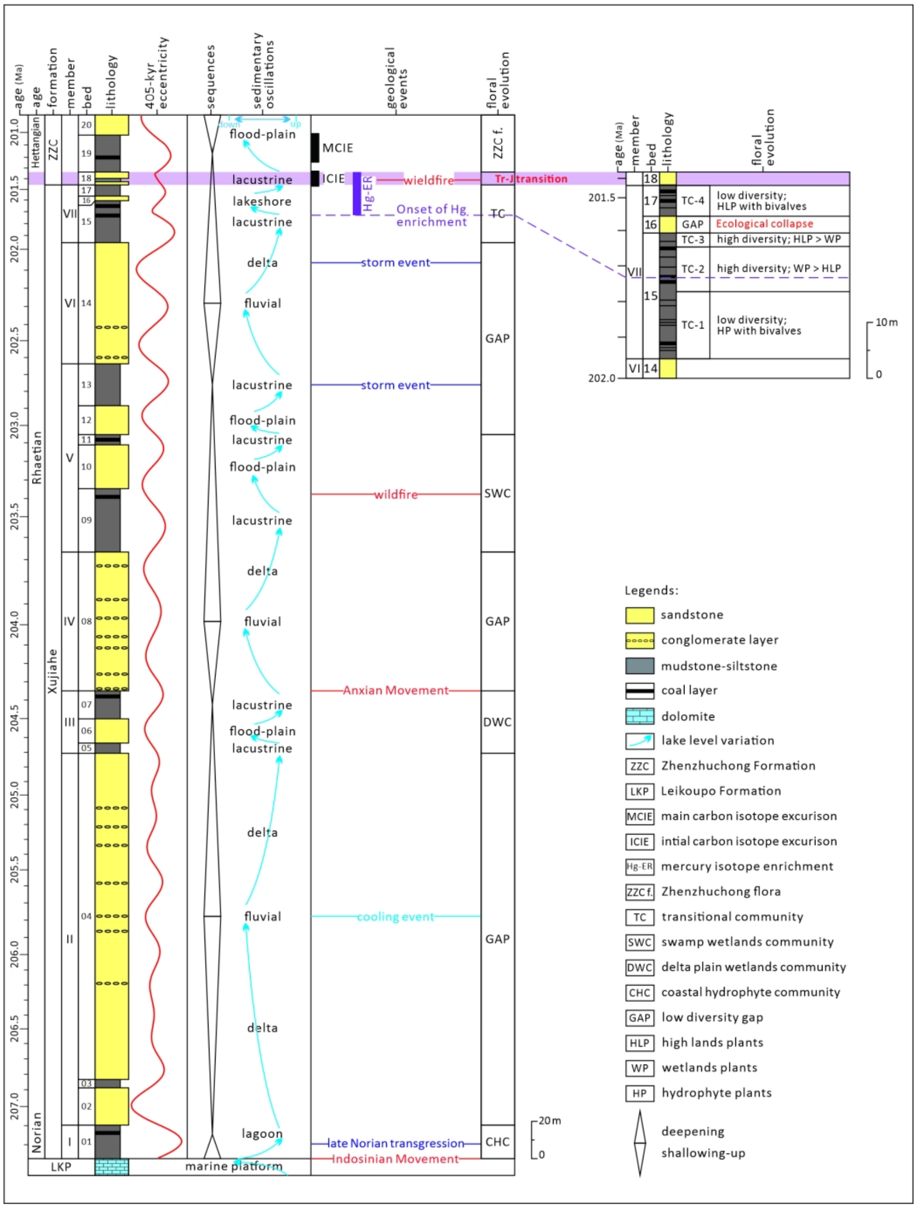

162x214mm (300 x 300 DPI)

Supplementary Information Text for

Oscillations of a fluvial-lacustrine system and its ecological response in the Late Triassic, northeast Sichuan Basin, China

Ning Lu, Yongdong Wang*, Yuanyuan Xu, Liqin Li, Xiaoping Xie, Mihai Emilian Popa*, Hongyu Chen, Micha Ruhl, Wolfram Michael Kürschner

*** Correspondence:**

Yongdong Wang: ydwang@nigpas.ac.cn;

Mihai Emilian Popa: mihai@mepopa.com

This PDF file includes:

Tabel S1. List of species of the Late Triassic Xujiahe Flora from the Qilixia section and its environs, NE Sichuan Basin, China.

Table S1. List of species of the Late Triassic Xujiahe Flora from the Qilixia section and its environs, NE Sichuan Basin, China.

Family*	Genus	Species	Stratigraphic occurrence		
			M. III	M. V	M. VII
	Equisetites Sternberg**	*E. intermedius* Erdtman	+	+	
		E. koreanicus Konno			+
		E. laevis Halle	+		
		E. sarrani Zeiller	+	+	
		E. scanicus (Sternberg) Halle	+	+	+
		E. sp. 1	+		
		E. sp. 2			+
	Equisetostachys Jongmans	*E.* sp.	+	+	+
	Neocalamites Halle	*N. carcinoides* Harris	+	+	+
		N. carrerei (Zeiller) Halle			+
		N. hoerensis (Schimper) Halle			+
		N. sp.***			
	Schizoneura Schimper et Mougeot	*S.* sp.			+
	Annulariopsis Zeiller	*A.* cf. *A. inopinata* Zeiller	+		+
	Taeniocladopsis Sze	*T. rhizomoides* Sze			+
Marattiaceae	*Danaeopsis* Heer	*D. fecunda* Halle	+		
Osmundaceae	*Todites* Seward	*T. kwangyuanensis* (Li) Ye et Chen	+		+
		T. shensiensis (P'an) Sze		+	
	Osmundopsis Harris	*O. plectrophora* Harris	+	+	
Cynepteridaceae	*Cynepteris* Ash	*Cynepteris lasiophora* Ash			+
Dipteridaceae	*Clathropteris* Brongniart	*C. meniscioides* Brongniart	+		
		C. mongugaica Srebrodolskaya			+
		C. platyphylla (Goeppert) Schenk		+	+
		C. tenuinervis Wu			+
	Dictyophyllum Lindley et Hutton	*D. nathorsti* Zeiller	+		+
	Hausmannia Dunker	*H. ussuriensis* Kryshtofovich			+
	Thaumatopteris (Goeppert) Nathorst	*T. nipponica* Oishi			+

	Cladophlebis Brongniart**	*C. calcarifomis* Chu		+	
		C. denticulata (Brongniart) Nathorst			+
		C. integra (Oishi et Takahashi) Frenguelli			+
		C. scariosa Harris			+
		C. cf. *C. kaoiana* Sze	+	+	+
		C. cf. *C. nalivkini* Thomas		+	
		C. sp.		+	
	Chiropteris Kurr	*C.? Yuani* Sze			+
		C.? sp.			+
	Rhizomopteris Schimper	*R.* sp.			+
	Thinnfeldia Ettingshausen	*T. rigida* Sze			+
	Compsopteris Zalessky	*C. acutifida* Ye et Chen			+
	Pachypteris Brongniart	cf. *P. chinensis* Hsü et Hu			+
	Ptilozamites Nathorst	*P. chinensis* Hsü			+
	Pterophyllum Brongniart	*P. angustum* (Braun) Gothan			+
		P. astartense Harris			+
		P. costa Ye et Xu			+
		P. exhibens Li			+
		P. pinnatifidum Harris	+		+
		P. ptilum Harris		+	+
		P. sinense Li	+		+
		P. subaequale Hartz			+
		P. tietzei Schenk			+
	Anomozamites Schimper	*A. loczyi* Schenk	+		
		A. marginatus (Unger) Nathorst			+
	Zamites Brongniart	*Z. jiangxiensis* Yao et Lih		+	+
		Z. sinensis Sze			+
	Otozamites Braun	cf. *O. ptilophylloides* Barbard et Miller			+
	Sinoctenis Sze	*S. calophylla* Wu et Lih			+
	Nilssonia Brongniart	*N. furcata* Chow et Tsao			+
	Ctenis Lindley et Hutton	*C. chaoi* Sze		+	

		C. denticulata Ye et Huang	+		
		C.? *mirabilis* Ye et Huang	+		
		C. nilssoni (Nathorst) Harris			+
		C. yamanarii Kawasaki			+
		C. cf. *C. yungjenensis* Chen			+
	Anthrophyopsis Nathorst	*A. venulosa* Chow et Yao emend Xu, Popa et Wang	+		+
	Ctenozamites Nathorst	*C. cycadea* (Berger) Schenk		+	
	Pseudoctenis Seward	*P. xiphida* Ye et Huang			+
	Doratophyllum Harris	*D.* cf. *D. astartensis* Harris			+
		D. decoratum Li			+
		D. hsuchiahoense Li			+
		D. sp.			+
	Cycadolepis Saporta	*C. corrugata* Zeiller			+
	Vardekloeftia Harris	*V. sulcata* Harris			+
	Bucklandia Presl	*B. minima* Ye et Peng			+
		B. sp.			+
	Ginkgoites Seward	*G.* cf. *G. huttoni* (Sternberg) Seward			+
	Baiera Braun	*B. elegans* Oishi			+
		B. cf. *B. furcata* (L.et H.)Braun			+
		B. cf. *B. muensteriana* (Presl) Heer			+
	Sphenobaiera Florin	*S.* cf. *S. spectabilis* (Nathorst) Florin			+
	Eretmophyllum Thomas	*E.* sp.			+
	Pseudotorellia Florin	*P.* sp.			+
	Hartzia Harris	*H. tenuis* Harris			+
	Sphenarion harris	cf. *S. leptophylla* (Harris) Harris			+
	Leptostrobus Heer	*L.* cf. *L. cancer* Harris			+
	Ixostrobus Raciborski	*I. lepidus* (Heer) Harris	+		+
		I. sp.			+
	Stenorachis Saporta	*S.* cf. *konianus* Oishi et Huzioka		+	
	Stachyopitys Schenk	*S.* sp.	+		
	Elatocladus Halle	*E.* sp.			+
	Pityophyllum Nathorst	*P. nordenskioildi* (Heer) Nathorst			+
	Podozamites Braun	*P. distans* (Presl) Braun		+	+
		P. mucronatus Harris			+

		P. schenki Heer			+
		P. cf. *P. astartensis* Harris			+
		P. cf. *P. griesbachi* Seward		+	
		P. cf. *P. issykkulensis* Genkina			+
		P. cf. *P. punctatus* Harris			+
		P. cf. *P. stewartensis* Harris			+
		P. sp.***			
	Ferganiella Prynada	*F. podozamioides* Lih	+		
	Lindleycladus Harris	*L.* cf. *L. lanceolatus* (L. et H.) Harris	+		
	Schizolepis Braun	*S. gracilis* Sze			+
	Cycadocarpidium Nathorst	*C. erdmanni* Nathorst		+	+
		C. swabii Nathorst (s.l.)	+	+	
	Nagatostrobus Konno	*N. linearis* Konno		+	+
	Ourostrobus Harris	*O.* cf. *O. nathorsti* Harris			+
	Strobilites Lindley et Hutton	*S.* sp.			+
	Samaropsis Geoppert	*S.* sp.			+
	Taeniopteris Brongniart	*T.* sp.			+
	Radicites Potonie**	*R.* spp.		+	

*Uncertain or controversial systematic affinities are not shown.

** *Equisetites* sp., *Cladophlebis* sp., *Podozamites* sp. and *Radicites* sp. also occurred in the Member I.

*** *Neocalamites* sp. and *Podozamites* sp. also occurred in the Member II.

Referrences

Huang, Q., and Lu, S. (1992). The Primary Studies on the Palaeoecology of the Late Triassic Xujiahe Flora in Eastern Sichuan. Earth Science-Journal of China University of Geosciences 17(3), 329-335.

Lu, N., Xie, X., Wang, Y., and Li, L. (2015). The Analysis of Sedimentary Environmental Evolution of the T3x/T2l Boundary Transition in Qilixia of Xuanhan, Sichuan. Acta Sedimentologica Sinica 33(6), 1149-1158.

Lu, N. (2019). Changes in sedimentary environment and terrestrial paleoecology across the Triassic-Jurassic transition in eastern Sichuan Basin. doctoral thesis, University of Science and Technology of China.

Wang, Y., Fu, B., Xie, X., Huang, Q., Li, K., Li, G., et al. (2010). The Terrestrial Triassic and Jurassic Systems in the Sichuan Basin, China. Hefei, China: University of Sicence and Technology of China Press.

Wu, S. (1999). Upper Triassic plants from Sichuan. Bulletin of Nanjing Institute of Geology and Palaeontology, Academia Sinica (14), 1-69.

Yang. X. (1978). Mesozoic Plants, In: Institute of Geology of Southwest China (Ed.). The Palaeontological Atlas of Southwest China: Sichuan (vol. II). Beijing: Geological Publishing House. p. 469-534.

Ye, M., Liu, X., Huang, G., Chen, L., Peng, S., et al. (1986). Late Triassic and Early-Middle Jurassic Fossil Plants from Northeastern Sichuan. Hefei: Anhui Science and Technology Publishing House.

Zhou, N., Xu, Y., Li, L., Lu, N., et al. (2021). Pattern of vegetation turnover during the end-Triassic mass extinction: Trends of fern communities from South China with global context. Global and Planetary Change 205, 103585.

Conflict of Interest

The authors declare that the research was conducted in the absence of any commercial or financial relationships that could be construed as a potential conflict of interest.